

UNIVERSITY OF GRANADA



**EXPERIMENTAL CONFIGURATION TO DETERMINE
THE REAL PARAMETER β IN PMMA AND CFRP
WITH THE FINITE AMPLITUDE METHOD**

Author:

Antonio Manuel Callejas Zafra

Supervisor:

Dr. Guillermo Rus Carlborg

Master of Structures
Department of Structural Mechanics and Hydraulic Engineering,
University of Granada
Granada (Spain)

July 2014

Abstract

Parameters to measure nonlinearity (nonlinear parameter β) in polymethylmethacrylate (PMMA) and carbon fiber reinforced polymer (CFRP) materials have been determined with nonlinear ultrasound (NLUS). The nonlinear parameter β has been determined using the variation of the Finite Amplitude Method (FAM) with harmonic generation. Using this as a reference, it has been deduced the experimental configuration necessary to measure this nonlinear parameter in a correct and feasible way. Excitation level, frequency of the wave generated, number of cycles analysed and the distances transducer-specimen and specimen-hydrophone have been determined in both materials. The second contribution is a semi-analytical model that allows to obtain the real nonlinear parameter β in materials by removing water contribution and considering geometric and viscous attenuation, using the measures obtained in an immersion tank. Finally, an application of this model has been carried out in PMMA in order to determinate the real nonlinear parameter β in this material.

Keywords: nonlinear ultrasound, nonlinear parameter β , Finite Amplitude Method (FAM), harmonic generation, attenuation.

Resumen

Los parámetros necesarios para medir la no linealidad (parámetro β) en materiales como polimetilmetacrilato (PMMA) y fibra de carbono (CFRP), han sido determinados utilizando la técnica de ultrasonidos no lineales. Se ha determinado el parámetro no lineal β usando el Método de Amplitud Finita con la generación de armónicos. Usando esto como referencia, se ha deducido la configuración experimental necesaria para medir el parámetro no lineal de una forma correcta y fiable. El nivel de energía, la frecuencia de la onda generada, el número de ciclos analizados y las distancias transductor-espécimen y espécimen-hidrófono han sido determinadas en ambos materiales. La segunda contribución es un modelo semi-analítico que permite obtener este parámetro no lineal en diferentes materiales, eliminando la contribución no lineal del agua y considerando las atenuaciones geométrica y viscosa, usando las medidas obtenidas en un tanque de inmersión. Finalmente, se ha llevado a cabo una aplicación con el material PMMA para determinar el parámetro no lineal β real de dicho espécimen.

Palabras clave: ultrasonidos no lineales, parámetro no lineal β , Método de Amplitud Finita (MAF), generación de armónicos, atenuación.

Acknowledgements

First of all, I would like to thank the responsible for the direction of my research and head of Nondestructive Evaluation Laboratory of the Department of Structural Mechanics and Hydraulic Engineering, Dr. Guillermo Rus Carlborg for his permanent dedication to the investigation and for teaching and passing me down this vision, for his patience, rigor and constructive suggestion over the course of this year.

Secondly, I would like to thank all my colleagues of the Nondestructive Evaluation Laboratory for making the everyday life at the laboratory enjoyable and for their help and advices.

And finally, I thank to my family for the support and help during the most difficult moments.

Contents

Abstract	i
Resumen	ii
Acknowledgements	iii
Contents	iv
List of Figures	vi
List of Tables	viii
1 Introduction	1
1.1 Context and Motivation	1
1.2 Research Objectives	3
1.3 Outline of Contributions	4
1.4 Literature Review	5
1.5 Theoretical Background	9
2 Methodology	11
2.1 Experimental Setup	11
2.2 Devices Description	13
2.3 Materials Description	16
2.4 Variables	17
2.5 Theoretical Foundations to Determine the Real Parameter β Considering Geometric and Viscous Attenuation	19
2.5.1 Solution	20
2.6 Semi-Analytical Approach	23
3 Results	27
3.1 PMMA Results	27
3.1.1 Excitation Level	27
3.1.2 Frequency	29
3.1.3 Cycles and Distance	29
3.1.4 Selected Parameters	31
3.2 CFRP Results	33

3.2.1	Excitation Level	33
3.2.2	Frequency	33
3.2.3	Cycles and Distance	36
3.2.4	Selected Parameters	38
3.3	Application of the Semi-Analytical Approach with PMMA Specimen . . .	39
4	Conclusions and Future Works	44
A	Matlab Codes	46
	Bibliography	56

List of Figures

2.1	Experimental set-up.	12
2.2	Wave generator.	13
2.3	Amplifier.	13
2.4	Oscilloscope.	14
2.5	Preamplifier.	14
2.6	Hydrophone.	14
2.7	Hydrophone sensitivity curve.	15
2.8	Transducer.	15
2.9	PMMA specimen.	16
2.10	CFRP specimen.	16
2.11	Scheme of inclusion of out of beam components as geometrical dispersion.	19
2.12	Semi-analytical approach used to extract the nonlinear material's properties from the measurements.	23
2.13	Determination of the β parameter and geometric attenuation in water layer 2 without specimen.	24
2.14	Determination of the geometric attenuation between A and B points without specimen.	24
2.15	Determination of the fundamental and second harmonic in B by propagating this values from C to B.	25
3.1	Plots beta versus distance specimen-hydrophone	28
3.2	Box-plot beta versus frequencies from 4 MHz to 7 MHz in steps of 0.1 MHz, to different distances.	30
3.3	Surface beta versus frequencies from 4 MHz to 7 MHz in steps of 0.1 MHz and distance from 0.5 mm to 30 mm.	31
3.4	Box-plot beta versus cycles from 4 MHz to 7 MHz in steps of 0.1 MHz, to different distances.	32
3.5	Plots beta versus distance specimen-hydrophone	34
3.6	Box-plot beta versus frequencies from 4 MHz to 7 MHz in steps of 0.1 MHz and 320mV, to different distances.	35
3.7	Surface beta versus frequencies from 4 MHz to 7 MHz in steps of 0.1 MHz and distance from 0.5 mm to 50 mm.	36
3.8	Box-plot beta versus cycles from 4 MHz to 7 MHz in steps of 0.1 MHz and 320mV, to different distances.	37
3.9	Semi-analytical approach used to extract the nonlinear material's properties from the measurements in PMMA specimen.	39
3.10	Determination of the β parameter and geometric attenuation in water layer 2 without specimen.	40

3.11 Determination of the geometric attenuation between A and B points without specimen.	41
3.12 Determination of the fundamental and second harmonic in B by propagating this values from C to B.	42

List of Tables

3.1	Selected parameters to measure the nonlinear parameter in PMMA	31
3.2	Selected parameters to measure the nonlinear parameter in CFRP	38

Chapter 1

Introduction

1.1 Context and Motivation

Nondestructive Evaluation is an emerging technique which aims to characterize the material damage without altering the material analyzed. Ultrasound is a non-destructive technique widely used today which is characterized by its low cost and potential for damage detection.

Initially, ultrasonic techniques were used to characterize homogeneous and isotropic materials. Very reliable damage parameters were obtained with these techniques, although numerous linear hypotheses were considered. These techniques are known as linear ultrasonic methods. When the need arose to address complex problems, consideration of these assumptions became a problem. The situation led to the development of new models and theories of nonlinear ultrasound (classical nonlinear elasticity, hertzian contact, nonlinear dissipation ... [1]), known as nonlinear ultrasonic methods to characterize inhomogeneous materials or materials with layers. Methods that not only use the first harmonic, but the second and even third harmonic to quantify the damage in complex materials.

Within the field of ultrasonic nonlinearity, different experimental techniques have been developed to measure the nonlinearity: Finite Amplitude Method (based on harmonic generation [2]), Nonlinear Elastic Wave Spectroscopy (based on principles of resonance [3]), including Nonlinear Resonant Ultrasound Spectroscopy (NRUS), and Nonlinear Wave Modulation Spectroscopy (NWMS) and Dynamic Acousto-Elasticity (DAE) [4].

In this thesis, for determining the real nonlinear parameter beta in materials such as polymethylmethacrylate (PMMA) and carbon fiber reinforced polymer (CFRP), the method of finite amplitude has been used. This method has been used for several reasons: (1) is the most common method used for the determination of this parameter in solids and

fluids and for that reason, there are many references concerning the method in which to draw and (2) it does not require the use of a complicated experimental setup, such as a high-pressure cell.

The correct determination of the nonlinear parameter β requires signals with little noise as possible. This is essential to really know the nonlinear characteristics of any material. Previous studies found too high β parameter for PMMA, due to reflections inside the PMMA sample [5]. Motivated by this, a parametric experimental setup is proposed to measure the nonlinear parameter β in polymethylmethacrylate and carbon fiber reinforced polymer in an immersion tank. Currents methods for ultrasonically quantifying the constitutive nonlinearity parameter β in materials do not consider attenuation in water. To overcome this, the nonlinear wave propagation equations are rigorously presented and enriched with the concept of geometrical dispersion, in order to consider viscous and geometric attenuation in materials (PMMA and CFRP) and fluids (water in this case).

1.2 Research Objectives

Damage prediction in materials is a very important issue today. Ultrasonic nondestructive evaluation allows to obtain parameters characterizing damage in homogeneous and inhomogeneous materials. However, due to their complexity, inhomogeneous materials such as layered materials require special care in signal interpretation. An appropriate configuration to obtain the nonlinear parameter in materials is the ultimate goal of this thesis. To approach this objective, two concrete objectives are formulated on the basis of some hypothesis to validate or falsify, listed below.

In the literature, the nonlinear parameter beta has been determined in a immersion tank under different configurations, some of which have as result incorrect values of this parameter due to reflection inside the material.

→ *Research hypothesis 1:* measurements to obtain the nonlinear parameter in a immersion tank can be obtained in a more correct way by eliminating any noise source.

Obtaining a correct nonlinear parameter in materials requires the elimination of the nonlinearity introduced by the medium used for the wave propagation, in this case is water.

→ *Research hypothesis 2:* the real nonlinear parameter beta could be more accurately obtained by subtracting different nonlinear contributions in measures.

1.3 Outline of Contributions

The thesis intends to provide suitable solutions to the two research questions outlined in **Section 1.2**, with the main objective of the determination of an appropriate configuration to obtain the real nonlinear parameter in materials. The methods and experiments are outlined in this chapter.

Research question 1:

Measurements to obtain the nonlinear parameter β in a immersion tank can be obtained in a more correct way by eliminating any noise source.

To investigate this research question, an appropriate experimental configuration has been found in order to obtain a signal without noise. In **Section 2.1** an experimental set-up has been described. The devices used in the configuration are explained in **Section 2.2**. In this thesis two materials (PMMA and CFRP (**Section 2.3**)) have been studied to obtain the nonlinear parameter. Measured signals obtained have been used to determine the effective nonlinear parameter β . This is an effective parameter because have been considered water, electronic and material nonlinearities. The theory to get this nonlinear parameter is shown in **Section 1.5**. Finally, PMMA and CFRP results are explained in **Sections 3.1** and **3.2** respectively

Research question 2:

The real nonlinear parameter beta could be more accurately obtained by subtracting different nonlinear contributions in measures.

To deal with this question, a suitable scheme has been considered in order to remove water contribution in parameter β (**Section 2.6**). The theory to obtain the parameter β , considering viscous and geometric attenuation is shown in **Section 2.5**. Finally, an application example have been performed to obtain the real nonlinear parameter β in a PMMA sample **Section 3.3**.

1.4 Literature Review

Nonlinearity is a property of a medium by which the shape and amplitude of a signal at a location are no longer proportional to the input excitation. In general, the propagation of a finite-amplitude plane wave through an acoustic nonlinear medium introduces distortions, resulting in the generation of higher harmonics. The acoustic nonlinearity observed as appearance of a harmonics in ultrasound propagation is a consequence of the deviation from perfect linear elasticity of the compressional mechanical constitutive law. There are some kind of theories based on the nonlinearity of the ultrasound, and this could be organized into [1] :

- *Classical nonlinear elasticity.* Which is based on the study of the second and third harmonic of the ultrasonic wave.
- *Bilinear stiffness, breathing cracks and clapping contacts.* Based on the lateral motion of cracks faces leading to crack opening/closing.
- *Hysteresis.* It follows different stress-strain curves in loading and unloading.
- *Hertzian contact.* In such models, a crack is considered as a contact of two elastic, frictionless half spaces.
- *Nonlinear dissipation.*

These theories have been developed by many researchers in order to get some clear conclusion. Hysteretic theory has clearly been described by DAE (Dynamic Acousto Elasticity) [6–11]. The hysteretic behaviour has been expressed in terms of a different curve followed by the velocity propagation along the tensile-compression pump cycle. The higher the pump amplitude, the larger the hysteresis cycle.

Global damage was determined fast and efficient by Nonlinear Resonance Acoustic Spectroscopy (NRUS) [3]. Zacharias et al. [12] used the vibro-modulation method, which is based on the fact that a high-frequency ultrasound wave is modulated by a low-frequency vibration to arrive at the next conclusion: osteoporotic bone exhibits enhanced nonlinear behaviour compared to healthy bone.

Attending to the Classical Nonlinear Theory, used in this thesis, Finite Amplitude Method has been chosen for the reasons given in Chapter “Context and Motivation”.

Measuring the amplitudes of harmonics is commonly referred to as the finite-amplitude (FA) method, initially developed by Breazeale and Thompson (1963) [13]. The nonlinear coefficients are usually determined by measuring the second-harmonic generation and

sometimes higher harmonics, and can be used to characterize acoustic nonlinear properties of gases, liquids, and solids. For this technique, the through-transmission mode in immersion is usually preferred. Instead of using two transducers, it is opportune to replace the receiver by a needle hydrophone (with a nearly linear frequency response), in order to conveniently measure the second and higher-harmonics. A finite-duration burst of (nearly) pure tone - typically around 20 cycles long - is launched towards the specimen, and the progress of some stationary peaks near the end of the tone-burst is followed and selected to compute the Fast Fourier Transform (FFT), which then allows to obtain the second and higher-order harmonics amplitude.

Different wave types have been investigated with this technique, such as shear waves, surface acoustic waves (SAW), lamb waves [14], but above all longitudinal waves. Initially, bulk exploration using nonlinear longitudinal waves has attracted the attention of many authors. In the case of shear waves in pure isotropic materials, the second harmonic is impossible [15], so early damage is detectable since it makes them arise. Bulk waves experiences need double-sided access to the specimen, while SAW and lamb ones just need a single-side access. Notwithstanding, the pulse-echo technique using longitudinal waves has slightly been assessed in fluids [16], and metals [17, 18]. In such a case, the rebound on a pressure release boundary in most NDT applications and the double interaction make the signal interpretation particularly difficult [19].

The finite-amplitude technique has been shown to be useful for defect detection in ceramics [20], concrete structures [15, 21], composites [22], fatigue cracks in metals, such as steels, titanium, and aluminum alloys [23, 24]. Such defects are originated in internal stresses, micro-cracks, zero-volume disbonds, and usually precede the main cracking mechanisms and the failure of the material. Therefore, a considerable number of authors have been involved in laboratory experiments to show that cracks and imperfect interfaces can behave in a nonlinear fashion [25, 26], and have thus opened new opportunities to detect partially closed cracks that may not be identified by conventional linear methods.

The finite-amplitude method is a relatively straightforward technique to measure the second- and higher harmonic peaks, and thus obtain nonlinear elastic coefficients of a material. The low complexity of the experimental installation could make of this method a low-cost and valuable technology for in-situ industrial applications. Nonetheless, a practical extraction of the harmonics requires numerous efforts in minimizing the nonlinear distortions from electronic devices and in optimizing the reproducibility of the experiment. Indeed, several factors such as the size of the gap between the specimen and the receiver or the geometrical dispersion of the transducers (inherently related to the focal distance) may have a drastic influence on the measured nonlinear elastic coefficients, and should be analyzed carefully.

Using the Finite Amplitude Method (FAM), there are evidences about nonlinear parameter in fluids and PMMA, however there are little evidence in CFRP.

Nonlinearity in fluids has been investigated for a long time. The need to investigate this aspect is that several disciplines are interesting in this aspect, disciplines as medicine, engineering, etc. The first fluid that was investigated was air [27]. After that, some investigators studied nonlinearity in other fluids.

Several parameters, in order to measure the nonlinearity in fluids and solids (PMMA), have been developed, some of them are: β , B/A (A and B are parameters of the adiabatic expansion of pressure and the coefficient of the quadratic, respectively), Γ , etc. These parameters are based on the same principle, the relationship between the fundamental harmonic and the second harmonic, concretely between the fundamental and the square of the second harmonic (β).

Some researches have determined the nonlinear parameter B/A in water, liquid mixtures, water with high pressure and temperature, biological media, etc [28–35]. Water is the fluid that has been investigated more and it is the medium by which the wave propagates in an immersion tank. The propagation of the wave through this medium causes the generation of higher harmonics. Experimentally, the acoustic nonlinear parameter of water was determined, obtaining the following results: $\beta = 3.5 \pm 0.1$ [31], $B/A = 6.2 \pm 0.6$ [28] and $B/A = 5.2$ [30]. These values were determined at atmospheric conditions. The influence of pressure and temperature on the value was studied by Plantier et al. [32]. With high values of pressure, the nonlinear parameter increases and vice versa, also with high temperature, it is higher.

Other materials have been investigated less as biological samples. W. K. Law [34] determined for solutions of bovine serum albumin, of dextrans, of sucrose, of hemoglobin extracted from blood and for fresh whole blood the nonlinearity parameter B/A . Other authors, Gong Xiu-fen et al. [33] measured the same nonlinear parameter for several biological samples (ethanol, acetone, ethylene glycol, porcine whole blood and bovine whole blood). The conclusion that all these authors obtained was that the value of the nonlinear parameter B/A increase with solution concentration

Respect to polymethylmethacrylate (PMMA), there are few references about the nonlinear parameter β using the Finite Amplitude Method. Rus et al. [36] found $\beta = 10$ in undamaged PMMA. On the other hand, Renaud et al. [5] found $\beta = 14$ for Plexiglas (PMMA), whereas the usual value is 7.5. This overestimation was probably due to reflections inside the Plexiglas sample.

β values for the CFRP are hardly comparable, since this material may strongly depend upon the manufacture process, on the properties of each component, and on the laminate stacking sequence.

There is a gap within the experimental configuration in the measures in an immersion tank [5]. This field has not been considered by the researchers yet it is a very important subject. Idjimarene et al. [37] state that the nonlinear indicator is dependent on the position of the receiver, and it is sensitive to the level of noise. If the excitation has a small level the non-linearity observed is produced by the non-linearity of the noise ahead of the excitation, so there is a threshold where the non-linearity of the excitation is dominant. The configuration gained from the Rus et al. [34] paper is the basis of this work.

Currents methods for ultrasonically quantifying the constitutive nonlinearity parameter beta in materials do not consider attenuation in water [5, 36]. For this reason, there is another gap respect to the estimation of the correct nonlinear parameter β .

1.5 Theoretical Background

The aim of this chapter is to supply the theoretical basis for determining an effective nonlinear parameter β with measured signals in an immersion tank (details can be found in [36]). This theory will be used over the course of this thesis. Next, the theory to obtain the formula for calculating the effective nonlinearity parameter is shown.

By adopting the one-dimensional nonlinear equation of motion up to first-order nonlinearity:

$$\frac{\partial^2 u}{\partial t^2} = c_p^2 \frac{\partial^2 u}{\partial x^2} \cdot \left(1 - 2\beta \frac{\partial u}{\partial x} - \dots\right) \quad (1.1)$$

where c_p is the longitudinal wave velocity and β is the pressure-volumetric nonlinear parameter of first order.

The wave displacement can be written as:

$$u = u_1 + u_2 + \dots \quad (1.2)$$

where u_1 and u_2 denote the zero-order and first-order perturbations solutions, respectively. The zero order perturbation solution corresponds to the fundamental solution of the linear wave equation (that is, when $\beta = 0$). When considering a monochromatic plane wave propagating in a semi-infinite nonlinear elastic layer, the latter is given as:

$$u_1 = A_1 \sin(kx - \omega t) \quad (1.3)$$

where A_1 is the constant amplitude of the plane wave, k is the wave number, and ω is the angular frequency. The first-order perturbation equation is:

$$\frac{\partial^2 u_2}{\partial x^2} - \frac{1}{c_p^2} \frac{\partial^2 u_2}{\partial t^2} = 2\beta \frac{\partial^2 u_1}{\partial x^2} \frac{\partial u_1}{\partial x} \quad (1.4)$$

The solution approach for the particular solution of u_2 must be multiplied by a sufficiently large power of x to become linearly independent. Thus, a particular solution may be obtained by the method of variations of parameters,

$$u_2 = A(x) \sin(2(kx - \omega t)) + B(x) \cos(2(kx - \omega t)) \quad (1.5)$$

where $A(x)$ and $B(x)$ represent space-dependent amplitudes of the first-order perturbation solution.

Therefore, the solution of the first equation (1) in this section is:

$$u(x, t) = A_1 \sin(kx - \omega t) + \frac{1}{4} \beta k^2 A_1^2 x \cos(2(kx - \omega t)) \quad (1.6)$$

where the first-order perturbation solution is generated by the fundamental waves, whose amplitude accumulates with the propagation distance. From that solution, the nonlinear parameter of first-order β is derived as,

$$\beta = \frac{4A_2}{k^2 x A_1^2} \quad (1.7)$$

where A_1 is the fundamental amplitude and A_2 is the amplitude of the second harmonic, x is the distance transducer-hydrophone (the distance x includes three layers water-specimen-water, for this reason the parameter β is an effective parameter) and k is the wave number. The two harmonic amplitudes have been determined using a variation of the finite amplitude method with harmonic generation. The finite amplitude method provides information of the coefficient of nonlinearity, β , through the ratio between the amplitude of the fundamental and the second harmonic amplitude.

Chapter 2

Methodology

In this chapter, the experimental setup (Section 2.1) used to measure in an immersion tank is shown. After that, it is presented the devices description in Section 2.2. The specimens used in this thesis have the characteristics indicated in Section 2.3. In Section 2.4 the variables, in the context of the test, are described. Finally, the equation to determinate the real nonlinear parameter β and a semi-analytical approach are presented in Sections 2.5 and 2.6 respectively.

2.1 Experimental Setup

The specimens were excited with a range of frequencies around the center frequency of the transducer, to see how the nonlinearity varied with the range of frequencies. For each frequency, the wave generator sent various excitation energies that were amplified before reaching the transducer.

After that, the wave generated by the unfocused transducer (which transforms the electrical signal into acoustic signal), travelling in the immersion tank through the water to the specimen (PMMA or CFRP). This signal, which is attenuated by water and transmission coefficient water-specimen, interacts with the nonlinearity of the material, generating a wave rich in harmonics. After crossing the material, the wave travels back through the water layer to reach the hydrophone, which converts acoustic signal (wave) into an electrical signal, pre-amplified and displayed on the oscilloscope.

The specimen-hydrophone distance varies while keeping fixed the distance between the transducer and the specimen. Finally, the recorded signal is processed to obtain an apparent nonlinearity parameter which takes into account the electrical nonlinearity, water nonlinearity and specimen nonlinearity (figure 2.1).

The used method is called Harmonics Generation method, which consists on analysing the first and second harmonics generated by the materials in which the wave is propagated.

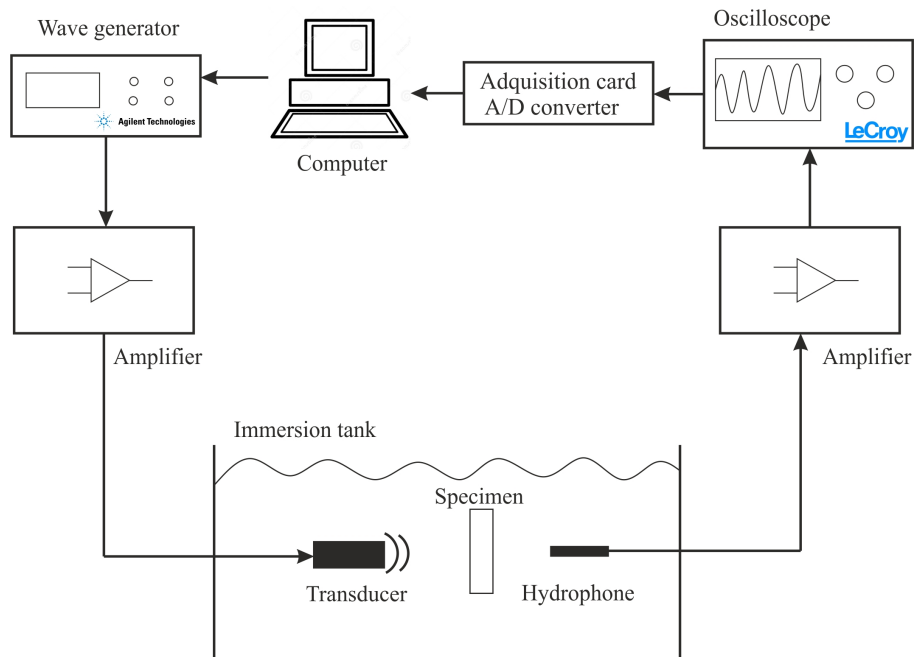


FIGURE 2.1: Experimental set-up.

2.2 Devices Description

The devices that have been used for conducting the tests are listed below.

- **Wave generator:** Agilent 33250 A, 80 MHz. (Figure 2.2)



FIGURE 2.2: Wave generator.

- **Amplifier:** Model 150 A 100 B, 150 Watts, 10 KHz-100 MHz. (Figure 2.3)



FIGURE 2.3: Amplifier.

- **Oscilloscope:** HDO 4034, 350 MHz, 2.5 GS/s. (Figure 2.4)
- **Preamplifier:** OLYMPUS ultrasonic preamplifier, Model 5676, 172 x 42.5 dB. (Figure 2.5)
- **Hydrophone:** ONDA, Model HNR-0500. (Figure 2.6)

This hydrophone has a sensitivity curve, depending on the frequency emitted, the hydrophone has different sensitivity. The curve can be observed in Figure 2.7.

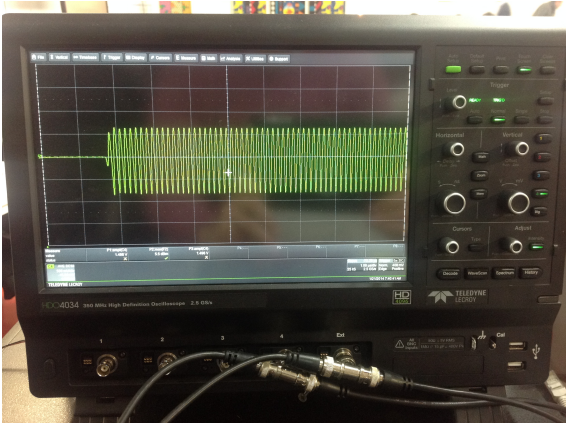


FIGURE 2.4: Oscilloscope.



FIGURE 2.5: Preamplifier.



FIGURE 2.6: Hydrophone.

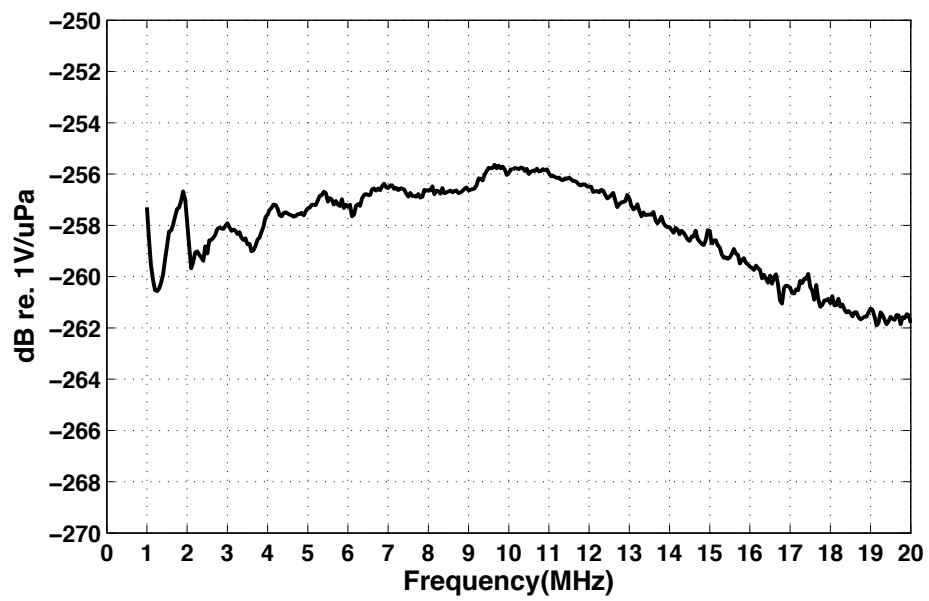


FIGURE 2.7: Hydrophone sensitivity curve.

- **Transducer:** Olympus panametrics-NDT, V310, 5 MHz/0.25", 686665. (Figure 2.8)



FIGURE 2.8: Transducer.

2.3 Materials Description

The completion of the trials was carried out with two specimens, polymethylmethacrylate (PMMA) and carbon fibre reinforced polymer (CFRP).

The first, PMMA (Figure 2.9), whose molecular formula is $C_5O_2H_8$, is the most transparent plastic, with a transparency of about 93%, a thickness of 20 mm and a density of 1190 kg/m^3 . Within two materials mentioned, this is a very homogeneous material against carbon fibre.



FIGURE 2.9: PMMA specimen.

The second material is CFRP (Figure 2.10), with a stacking sequence which corresponds to a $[0/90]_{4s}$ lay-up. It has a density of 1800 kg/m^3 and a thickness of 2 mm. This previous CFRF plate was previously subjected to stress - fatigue load in tension-compression (400,000 cycles).



FIGURE 2.10: CFRP specimen.

2.4 Variables

The variables used in this work are described at this point. These are explained in the context of the tests, and they are as follows:

- **Excitation level.** This is the excitation energy sent from the transducer to the hydrophone, going through the specimen (PMMA or CFRP). This is produced in the wave generator (Agilent 33250 A) and amplified 27.5 dB by the amplifier (Amplifier Research 150A 100B). Three excitation levels were considered: 320 mV, 240 mV and 160 mV. This choice is based on the previous experience for generating nonlinearity.
- **Frequency.** It is generated in the transmitter transducer. It depends on the type of transducer. The transducer used has a central frequency of around 5 MHz, so it was decided to do a frequency sweep around this central frequency. This sweep was done as follows: from 4 MHz to 7 MHz increasing that frequency by 0.1 MHz. It was expected to get a accurate information about the correct frequency.
- **Distance.** The distance was varied between specimen-hydrophone, while maintaining a fixed distance between the transducer-specimen. This last distance is established because of the effects of the near field. The distance specimen-hydrophone is varied from 0.5 mm to 50.5 mm. The step is defined in 1 mm. This movement can be automatized because of the mechanical arm of the immersion tank controlled in MATLAB with the correspondent libraries for controlling the step-by-step motors.
- **Specimen thickness.** This is important data for calculating the value of the non-linear parameter β . This was measured with a gauge to ensure this variable with more accuracy.
- **Sampling.** In the sampling, the acquisition card was adjusted with a number of points for each cycles by which the sampling frequency was integer. This was necessary because if this was not done, the FFT in MATLAB was not well done, and may have problems like aliasing and leakage. With this adjustment these problems were avoided.
- **Window variation.** This variable is the time window in which the ultrasonic wave arrives to the hydrophone until a certain number of cycles. Different windows for each frequency were got. This was done because it was necessary to adjust the number of points analysed by the acquisition card. It was taken the number of points divided by 10 (the number of points that represent the wave) and it was got the number of cycles that the windows are able to capture. The wave region varies

in the distance, so the variance was established with an estimation of the retardment with the wave arriving at the hydrophone.

- **Wave region.** The first part of the wave was analysed in that window, trying to avoid undesired interferences which distort the value of the non-linear parameter β . This region depends on the material, for PMMA it was analysed until 150 cycles, nevertheless in the CFRP laminates it was analysed the firsts 30 cycles.
- **Hydrophone sensitivity.** In order to obtain a value of efficient beta (with water and material), it is necessary to obtain the value of the fundamental and second harmonic and each one has a different value of frequency (double), this was corrected with the sensitivity curve of the hydrophone, and each harmonic was treated with different value of this sensitivity.
- **Alignment.** It is important the correct alignment between transducer and hydrophone because a little misalignment causes variations in the nonlinear parameter β .

2.5 Theoretical Foundations to Determine the Real Parameter β Considering Geometric and Viscous Attenuation

The contribution that this section shows is the determination of a relationship between the nonlinear parameter β and the amplitude of the fundamental and second harmonic in two points separated by a distance x , considering geometric and viscous attenuation. The theory that is presented in this section is in preparation to be published ("Dispersion independent measurement of ultrasonic nonlinearity", authors: Guillermo Rus Carlborg and Nicolas Bochud).

In order to solve the wave propagated by a transducer along the center of the path, the x_1 axis is chosen as aligned with the propagation path, and the transversal components of the displacements are neglected. Thus, the 3D problem of finding $(u_1(x_1, x_2, x_3, t), u_2(x_1, x_2, x_3, t), u_3(x_1, x_2, x_3, t))$ is reduced to a 1D problem of finding the displacement field $(u_1(x_1, t), 0, 0)$ whose solution will be found analytically.

A strict application of the former simplification leaves out the effect of the geometric dispersion on the propagation along the axis. This will be shown to be responsible for large deviations that drastically reduce the validity of the formula that relates β with the amplitude of the harmonics. To overcome this, a procedure to include the effect of the geometric dispersion into the 1D formulation is presented. To this end, the compatibility equation is modified to include the incoming or outgoing components from outside the center of the beam, as depicted in Figure 2.11.

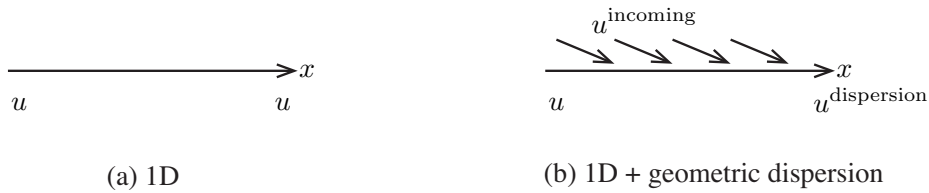


FIGURE 2.11: Scheme of inclusion of out of beam components as geometrical dispersion.

The incoming displacement u^{incoming} adds continuously a component to the original displacement, both in the x_1 direction. This can be expressed in the following differential form, where the addition happens gradually by a proportionality factor $2\alpha_g$,

$$\frac{du_1^{\text{dispersion}}(x_1, t)}{dx_1} = \frac{du_1(x_1, t)}{dx_1} + 2\alpha_g(x_1)u_1(x_1, t) \quad (2.1)$$

This can also be interpreted as a rate of change of the displacement $u^{\text{incoming}} - u$ with respect to the case without incoming wave, proportional to the amplitude u as,

$$\frac{d\left(u_1^{\text{dispersion}} - u_1\right)}{dx_1} = 2\alpha_g u_1 \quad (2.2)$$

The modified compatibility equation follows straightforwardly, including a new geometric dispersion term,

$$\varepsilon_{11} = u_{1,1} + 2\alpha_g u_1 \quad (2.3)$$

The compatibility, constitutive and equilibrium equations become, after assuming directional propagation $u_2 = 0 = u_3$,

$$\text{Compatibility:} \quad \varepsilon_{11} = u_{1,1} + 2\alpha_g u_1 = \varepsilon = -3v, \quad \varepsilon_{ij} = 0 \quad \forall (i, j) \neq (1, 1) \quad (2.4)$$

$$\text{Constitutive:} \quad \sigma_{kk} = -p = K\varepsilon + \frac{1}{2}\beta K\varepsilon^2 + \eta^v \dot{\varepsilon}, \quad \sigma_{ij} = 0 \quad \forall i \neq j \quad (2.5)$$

$$\text{Equilibrium:} \quad \rho \ddot{u}_1 = \sigma_{11,1} \quad (2.6)$$

The last four equations can be combined by substitution into a 1D nonlinear wave equation that includes geometrical dispersion correction,

$$\rho \ddot{u}_1 = K u_{1,11} + 2\alpha_g K u_{1,1} + \frac{1}{2}\beta K (u_{1,1}^2)_{,1} + \eta^v \dot{u}_{1,11} + O(\beta\delta) + O(\eta\delta) \quad (2.7)$$

where higher order terms $O(\beta\delta), O(\eta\delta)$ are negligible, and the four relevant terms at the right hand side are the linear compressibility, the geometrical dispersion, the nonlinear compressibility and the viscosity. For the sake of compactness, the direction index 1 will be dropped in the sequel, and the spatial derivative with respect to x_1 will be denoted by a tilde (i.e. $u_{1,1} = u'$).

2.5.1 Solution

The solution of equation 2.7 is sought as the sum of two attenuating traveling waves at velocity c with frequency ω and 2ω respectively, that stand for the fundamental due to linear propagation (u_0), and the harmonic generated by the nonlinearity (u_1 , which will be shown to be proportional to the degree of nonlinearity β). The complex exponential notation is adopted, where the phase component is omitted without loss of generality,

$$u = u_0 + u_1 \quad \begin{cases} u_0(x, t) = a(x)e^{i(kx - \omega t)} \\ u_1(x, t) = b(x)e^{2i(kx - \omega t)} \end{cases} \quad (2.8)$$

Substituting the decomposition above into equation 2.7 and neglecting terms of order $O(\beta^2)$ yields,

$$\frac{\rho}{K}(\ddot{u}_0 + \ddot{u}_1) = u_0'' + u_1'' + 2\alpha_g u_0' + 2\alpha_g u_1' + \frac{1}{2}\beta(u_0'^2)' + \frac{\eta^v}{K}\dot{u}_0'' + \frac{\eta^v}{K}\dot{u}_1'' \quad (2.9)$$

Recalling that the successive derivatives of the displacement components are,

$$\begin{aligned} \ddot{u}_0 &= -\omega^2 a e^{i(kx-\omega t)} \\ u_0' &= (ika + a^{\prime\prime}) e^{i(kx-\omega t)} \\ u_0'' &= (-k^2 a + 2ika' + a^{\prime\prime\prime}) e^{i(kx-\omega t)} \\ \dot{u}_0'' &= (i\omega k^2 a - 2\omega k a^{\prime\prime} - i\omega a^{\prime\prime\prime}) e^{i(kx-\omega t)} \\ (u_0'^2)' &= 2u_0' u_0'' = 2(-ik^3 a^2 - 3k^2 a a^{\prime\prime} + ika a^{\prime\prime\prime} + 2ik a^{\prime\prime 2} + a' a^{\prime\prime\prime}) e^{2i(kx-\omega t)} \\ \ddot{u}_1 &= -4\omega^2 b e^{2i(kx-\omega t)} \\ u_1' &= (2ikb + b^{\prime\prime}) e^{2i(kx-\omega t)} \\ u_1'' &= (-4k^2 b + 4ikb' + b^{\prime\prime\prime}) e^{2i(kx-\omega t)} \\ \dot{u}_1'' &= (8i\omega k^2 b - 8\omega k b^{\prime\prime} - i\omega b^{\prime\prime\prime}) e^{2i(kx-\omega t)} \end{aligned}$$

where some terms have been neglected since, for ultrasonic waves the wavenumber is much larger than the viscous or geometric dispersions, $k \gg \alpha_g, \alpha$ where the meaning of α and its relationship with a' and a'' will be understood in short.

Equation 2.9 should be fulfilled independently for terms propagating as $e^{i(kx-\omega t)}$ as for terms as $e^{2i(kx-\omega t)}$. This implies that the equation can be split into two equalities, of which the first one is,

$$\frac{\rho}{K}\ddot{u}_0 = u_0'' + 2\alpha_g u_0' + \frac{\eta^v}{K}\dot{u}_0'' \quad (2.10)$$

Given a fundamental excitation frequency ω , equation 2.10 is satisfied if $\frac{\rho}{K} = \frac{k^2}{\omega^2} = c^{-2}$, which defines the compressional wave velocity c and the wavenumber k . Equation 2.10 transforms into,

$$0 = 2ika' + 2\alpha_g ika + \frac{\eta^v}{K} ik^2 \omega a \quad \Rightarrow \quad a' = -\left(\alpha_g + \frac{\omega^2 \eta^v}{2\rho c^3}\right) a \quad (2.11)$$

which is a differential equation of first order, whose solution is, recalling that $K = \rho c^2$, and calling $\alpha = \frac{\omega^2 \eta^v}{2\rho c^3}$,

$$a(x) = a(0)e^{-(\alpha_g + \alpha)x} \quad (2.12)$$

The second equality, which groups terms propagating as $e^{2i(kx-\omega t)}$, is,

$$\frac{\rho}{K}\ddot{u}_1 = u_1'' + 2\alpha_g u_1' + \frac{\eta^v}{K}\dot{u}_1'' + \frac{1}{2}\beta(u_0^2)' \quad (2.13)$$

which, by removing common factors transforms into,

$$b' + (\alpha_g + 4\alpha)b = \frac{\beta k^2 a(x)^2}{4} \quad (2.14)$$

which is a differential equation of first order, of the form $y' + fy = g$, whose solution is somewhat more complex of the form $y = e^{-\int f dx} \left(\int g e^{\int f dx} dx + c \right)$.

$$b(x) = b(0)e^{-(4\alpha+\alpha_g)x} + \frac{\beta k^2 a(0)^2}{4(\alpha_g - 2\alpha)} e^{-(2\alpha+2\alpha_g)x} \quad (2.15)$$

The nonlinear parameter β , considering geometric and viscous attenuation is:

$$\beta = \frac{(b(x) - b(0)e^{-(4\alpha+\alpha_g)x})(4(\alpha_g - 2\alpha))}{k^2 a(0)^2 e^{-(2\alpha+2\alpha_g)x}} \quad (2.16)$$

However, if 2.13 is approximated by neglecting both viscous and geometric dispersion terms, the following solution is recovered,

$$b(x) = b(0) + \frac{\beta k^2 a(0)^2 x}{4} \quad (2.17)$$

If the initial amplitude of the second harmonic is assumed to be zero, the standard non-linearity estimator from the literature is recovered,

$$\beta = \frac{4b(x)}{k^2 a(x)^2 x} \quad (2.18)$$

2.6 Semi-Analytical Approach

After determining the correct parametric configuration to measure in an immersion tank, measures using the defined parameters have been carried out. The scheme used for determining the real parameter β is shown in Figure 2.12.

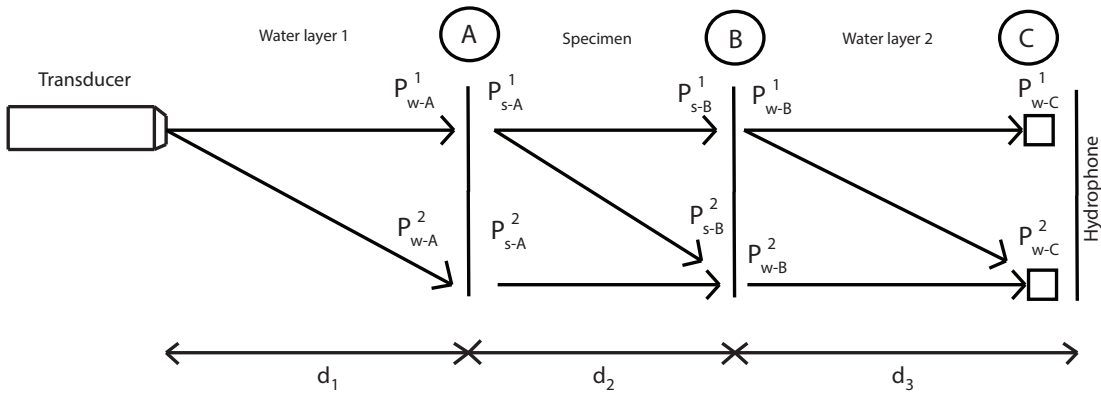


FIGURE 2.12: Semi-analytical approach used to extract the nonlinear material's properties from the measurements.

P is the pressure of the fundamental (superscript "1") and second harmonic (superscript "2"), "w" subscript indicates water, "s" indicates specimen and d_1 , d_2 and d_3 are distances.

The main aim is to determinate the fundamental and second harmonic pressure in A and B inside the specimen. With this values, the real nonlinear parameter β will be determinated. Before that, several steps are necessary.

The first step is to measure the fundamental and second harmonics pressure in A, B and C without specimen. With this values in B and C and using equations 2.12 and 2.15 it will be determinated the nonlinear parameter β in water and geometric attenuation in this water layer (Figure 2.13). Where "k" is the wave number, "α" is the viscous attenuation of water at the fundamental frequency ($\alpha = 20 \cdot 10^{-15} \cdot f^2$) [38] and "x" is the thickness of water layer 2.

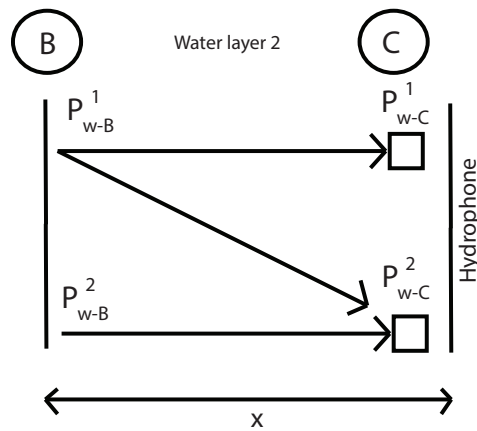


FIGURE 2.13: Determination of the β parameter and geometric attenuation in water layer 2 without specimen.

Then, using the same equations (2.12 and 2.15), geometric attenuation between A and B point is obtained without the presence of the specimen. Now, "x" is the distance between A and B.

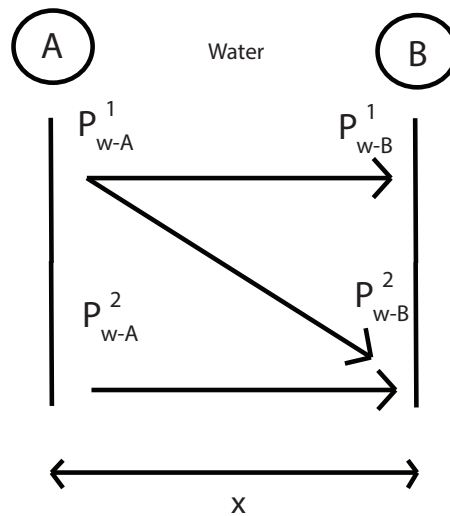


FIGURE 2.14: Determination of the geometric attenuation between A and B points without specimen.

The next step is to measure the fundamental and second harmonic pressure in C with the presence of the specimen. With this values and the values of nonlinear parameter β in water and geometric attenuation between B and C (previously calculated), it will be determined the amplitude of the fundamental and second harmonic in water and in B point (Figure 2.15), using the equations below:

$$a(0) = \frac{a(x)}{e^{-(\alpha_g + \alpha)x}} \quad (2.19)$$

$$b(0) = \frac{b(x) - \frac{\beta k^2 a(0)^2}{4(\alpha_g - 2\alpha)} e^{-(2\alpha + 2\alpha_g)x}}{e^{-(4\alpha + \alpha_g)x}} \quad (2.20)$$

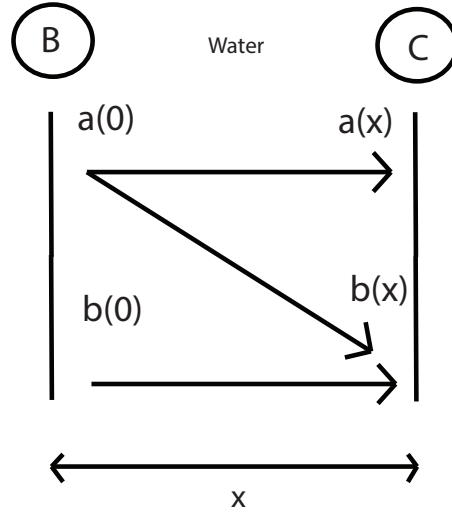


FIGURE 2.15: Determination of the fundamental and second harmonic in B by propagating these values from C to B.

The last step, before reaching the goal, is to obtain the values of the fundamental and second harmonic in A and B in specimen by multiplying these values in water for transmission coefficient water-specimen and specimen-water.

The transmission coefficient water-specimen and specimen-water are:

$$T_{w-s} = \frac{2Z_w}{Z_w + Z_s} \quad (2.21)$$

$$T_{s-w} = \frac{2Z_s}{Z_w + Z_s} \quad (2.22)$$

where Z_w and Z_s are the water impedance and the specimen impedance respectively.

Finally, with the values of fundamental and second harmonic in A and B in specimen and taking specimen attenuation from literature and geometric attenuation calculated before between A and B points, the real nonlinear parameter β in specimen, considering viscous and geometric attenuation, is calculated as follows:

$$\beta = \frac{(b(x) - b(0)e^{-(4\alpha_s + \alpha_g)x})(4(\alpha_g - 2\alpha_s))}{k^2 a(0)^2 e^{-(2\alpha_s + 2\alpha_g)x}} \quad (2.23)$$

where "x" is the specimen's thickness.

Chapter 3

Results

This chapter presents the parametric configuration obtained with two specimens: PMMA and CFRP (Sections 3.1 and 3.2). The final section of this chapter, Section 3.3, presents an application of the semi-analytical approach (Chapter 2 - Section 2.6) with PMMA specimen.

3.1 PMMA Results

3.1.1 Excitation Level

The excitation level was chosen in a first approximation with three different frequencies (5 MHz, 5.5 MHz and 6 MHz) around the center frequency of the transducer and three different energies (320 mV, 240 mV and 160 mV). A scan was performed in the wave emission direction, between 0.5 mm and 50.5 mm from the specimen.

In the figure 3.1 it can be observed that the nonlinear parameter β in the first centimetre has a very high variation. From there, variation is established around a value of beta and this stays until the end of the scanning. Results show the same pattern with a fixed frequency and for the different values of excitation level. By this reason, the excitation level of 320 mV was chosen because with a high excitation level, more nonlinearity level can be got, which implies that high order harmonics can be obtained with a higher level of energy.

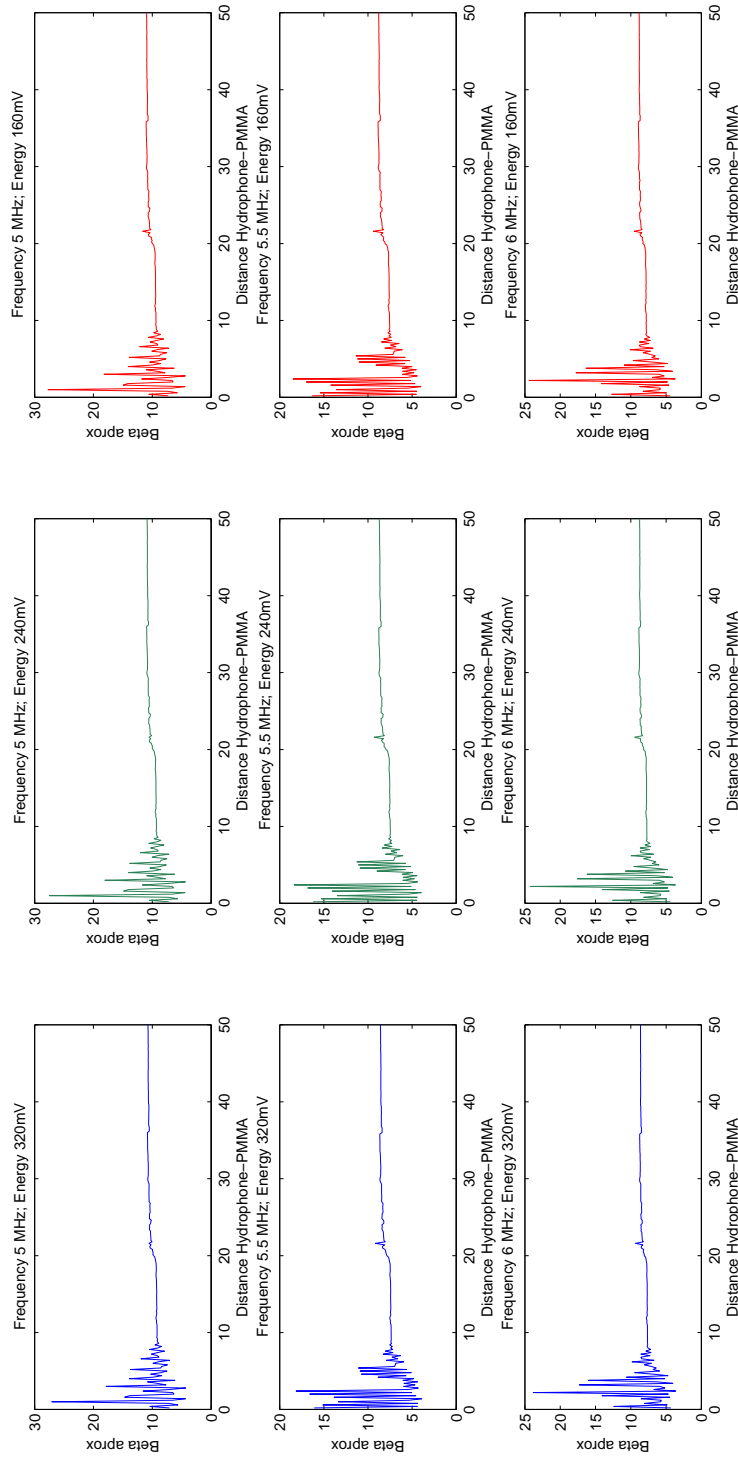


FIGURE 3.1: Plots beta versus distance specimen-hydrophone

3.1.2 Frequency

After choosing the excitation level, data from the tests with box-plots were studied. This sort of plot performs a data processing showing the mean and different percentiles of a group of data. In this case, it was analysed the value of the nonlinear parameter β in different intervals of distance specimen-hydrophone: between 0-10 mm, 10-20 mm and 20-30 mm, for 50 cycles¹ analysed and for different frequencies (4-7 MHz) to get information about which frequency has less variance around the central frequency of the transducer.

In the figure 3.2a it can be observed that there are a lot of dispersion (it can be appreciated by the red crosses, which are so far from the mean). A lower level of dispersion in the values of the nonlinear parameter β is shown in the figure 3.2b. The next figure 3.2c reveals a similar level of dispersion to the previous figure. Attending to the center frequency of the transducer, there are a range in which the beta mean is stable and the variance is low. It is between 5.7 MHz and 6.1 MHz and it was selected 5.9 MHz because it is a central value of this range and it is far from 6.2 MHz. In this last frequency the value of beta is very different to the previous and posterior frequency.

In Figure 3.3 it can be observed a surface in which z-axis represents beta values for a range of distances (0-30 mm) and a range of frequencies (4-7 MHz).

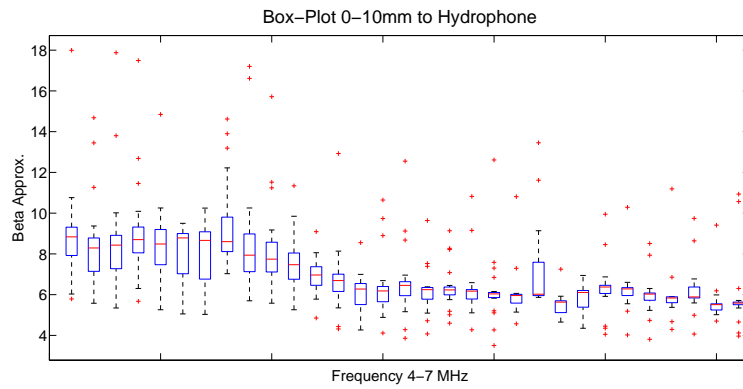
3.1.3 Cycles and Distance

With the excitation level and frequency fixed, it will be selected the distance between specimen and hydrophone and the number of cycles analysed in which the measure is suitable. In the figure 3.4a, with a distance between 0-10 mm from the specimen to the hydrophone it can be observed something similar to the figure 3.2a. There is too much dispersion because of the interferences caused by the proximity between specimen-hydrophone. This figure does not provide important information.

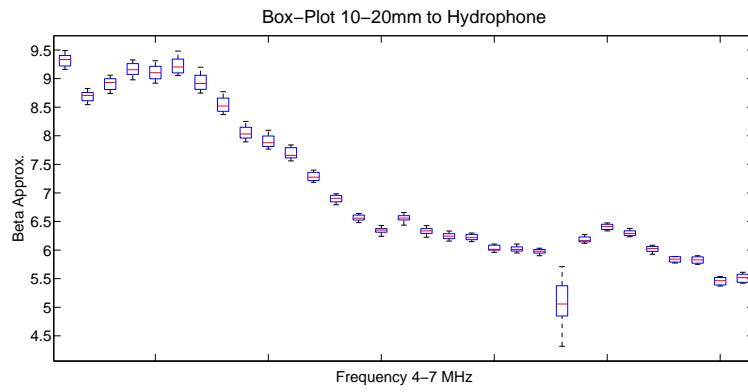
The two next figures 3.4b and 3.4c have a similar pattern. The only difference between them is that there are interferences observed with less distance (10-20 mm). This interference affects from 100 cycles analysed. This provides that this material is very homogeneous because it can be analysed a lot of cycles without interferences.

There is a wide range in which the mean of non-linear parameter is stable (between 50-80 cycles). It is reasonable to choose this range because there are not interferences and the mean of the nonlinear parameter β is approximately constant.

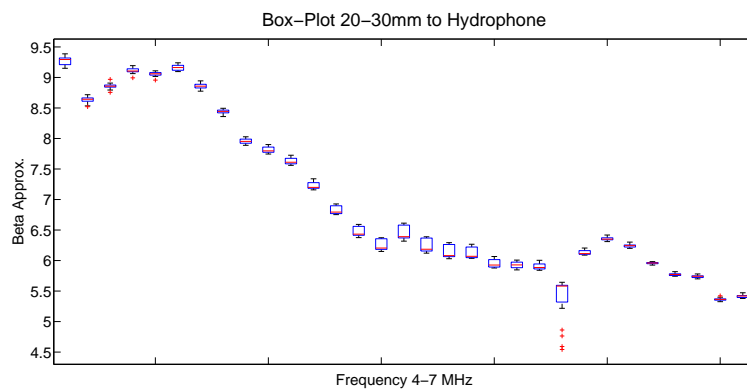
¹The number of cycles was elected because it was done this sort of plot with different number of cycles and the pattern was the same for different number of cycles.



(A) 0 -10 mm



(B) 10-20 mm



(c) 20-30 mm

FIGURE 3.2: Box-plot beta versus frequencies from 4 MHz to 7 MHz in steps of 0.1 MHz, to different distances.

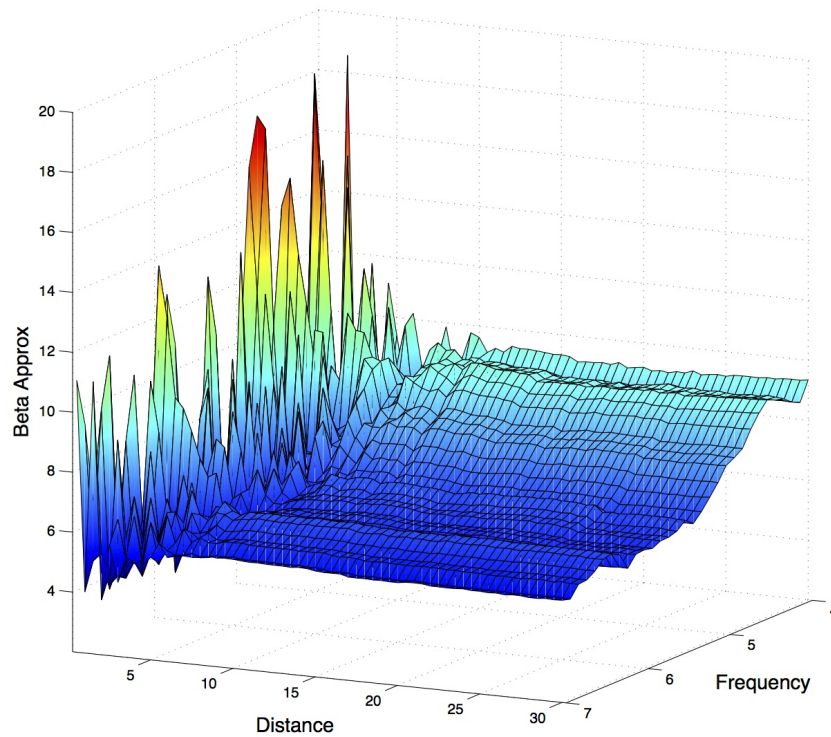


FIGURE 3.3: Surface beta versus frequencies from 4 MHz to 7 MHz in steps of 0.1 MHz and distance from 0.5 mm to 30 mm.

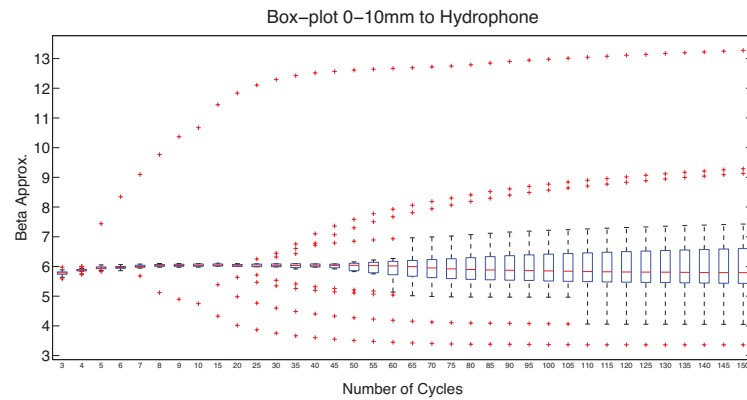
With the same box-plot it can be deduced the appropriate distance to do a feasible measure. This could be fitted in the range of 10-30 mm because in this range, for the number of cycles fixed previously, there are not interferences and the value of beta is stable. Within this range, for a shorter distance the attenuation is lower than in a longer distance. Therefore it is desirable to choose a distance near to 10 mm.

3.1.4 Selected Parameters

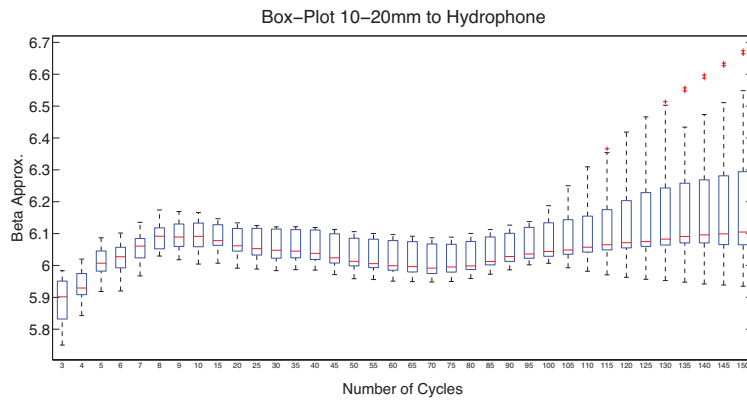
The parameters chosen for PMMA material are shown in the table below for the configuration established in this thesis:

Material	Excitation level (mV)	Frequency (MHz)	Cycles	Distance (mm)
PMMA	320	5.9	50-80	10-30

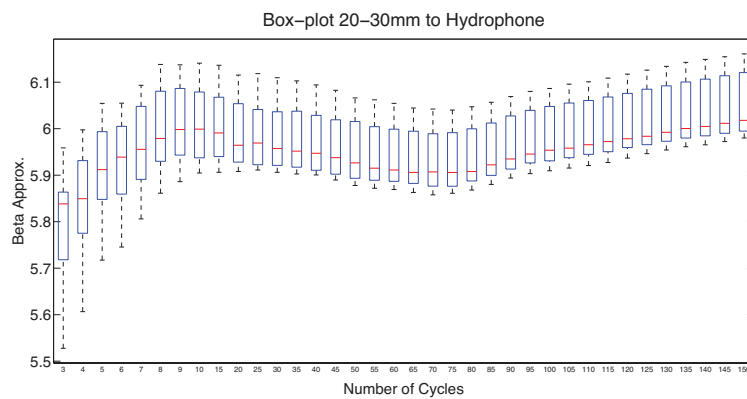
TABLE 3.1: Selected parameters to measure the nonlinear parameter in PMMA



(A) 0 -10 mm



(B) 10-20 mm



(c) 20-30 mm

FIGURE 3.4: Box-plot beta versus cycles from 4 MHz to 7 MHz in steps of 0.1 MHz, to different distances.

3.2 CFRP Results

3.2.1 Excitation Level

As with PMMA material, the excitation level was chosen in a first approximation with three frequencies (4 MHz, 5 MHz and 6 MHz), which are different from PMMA frequencies, around the center frequency of the transducer and three different energies (320 mV, 240 mV and 160 mV). A scan was performed in the wave emission direction, between 0.5 mm and 50.5 mm from the specimen.

In the figure 3.5 it can be observed that the nonlinear parameter β in the first two and a half centimetres has a very high variation. From there, variation is established around a value of beta and this stays until the end of the scanning. Results show the same pattern with a fixed frequency and for the different values of excitation level. By this reason, the excitation level of 320 mV was chosen by the same reason given with PMMA material.

3.2.2 Frequency

After choosing the excitation level, it was studied data from the tests with box-plots. It was analysed the value of the non-linear parameter β in different intervals of distance specimen-hydrophone: between 15-20 mm, 20-25 mm and 25-30 mm, for 4 and 20 cycles² analysed and for the different frequencies (4-7 MHz) to get information about which frequency has less variance around the central frequency of the transducer.

In the figure 3.6a it can be observed that there are a lot of dispersion with 4 and 20 cycles. In the next figure 3.6b, there is also dispersion although less than in the distance of 15-20 mm. On the other hand, in the third image 3.6c, the dispersion is lower than in the previous two images. It can be observed that with 20 cycles the values of nonlinear parameter β varies greatly with different frequencies than with both frequencies. With 4 cycles the values of β with the frequency follow the same pattern for the three different distances. For 4 cycles, the value of the frequency for which the value of beta converges after several tests is 5.8 MHz.

In Figure 3.7 it can be observed a surface in which z-axis represents beta values for a range of distances (0-50 mm) and a range of frequencies (4-7 MHz).

²The number of cycles was elected because it was done this sort of plot with different number of cycles and the pattern was different for different number of cycles because of the interferences. With 4 cycles there is not interference and with 20 cycles there is interference in the signal.

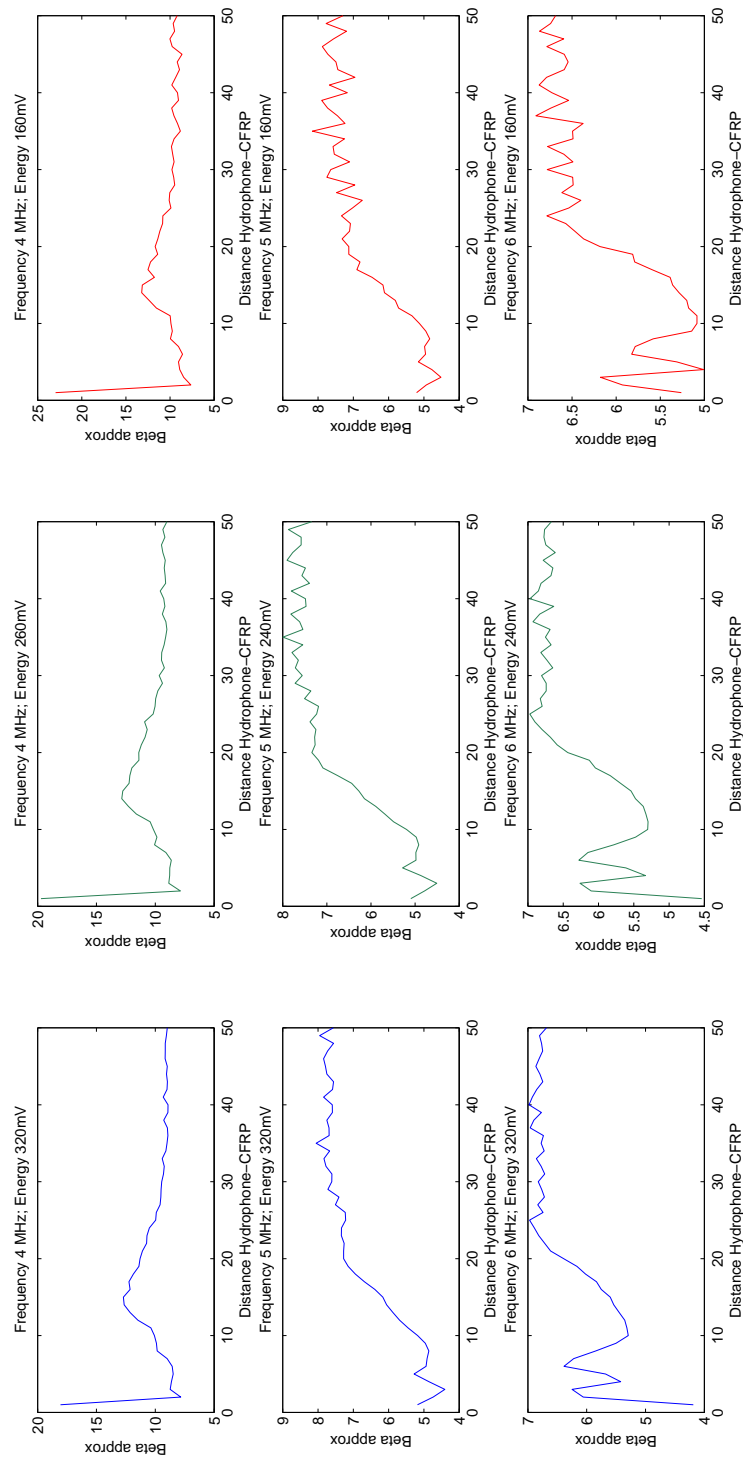


FIGURE 3.5: Plots beta versus distance specimen-hydrophone

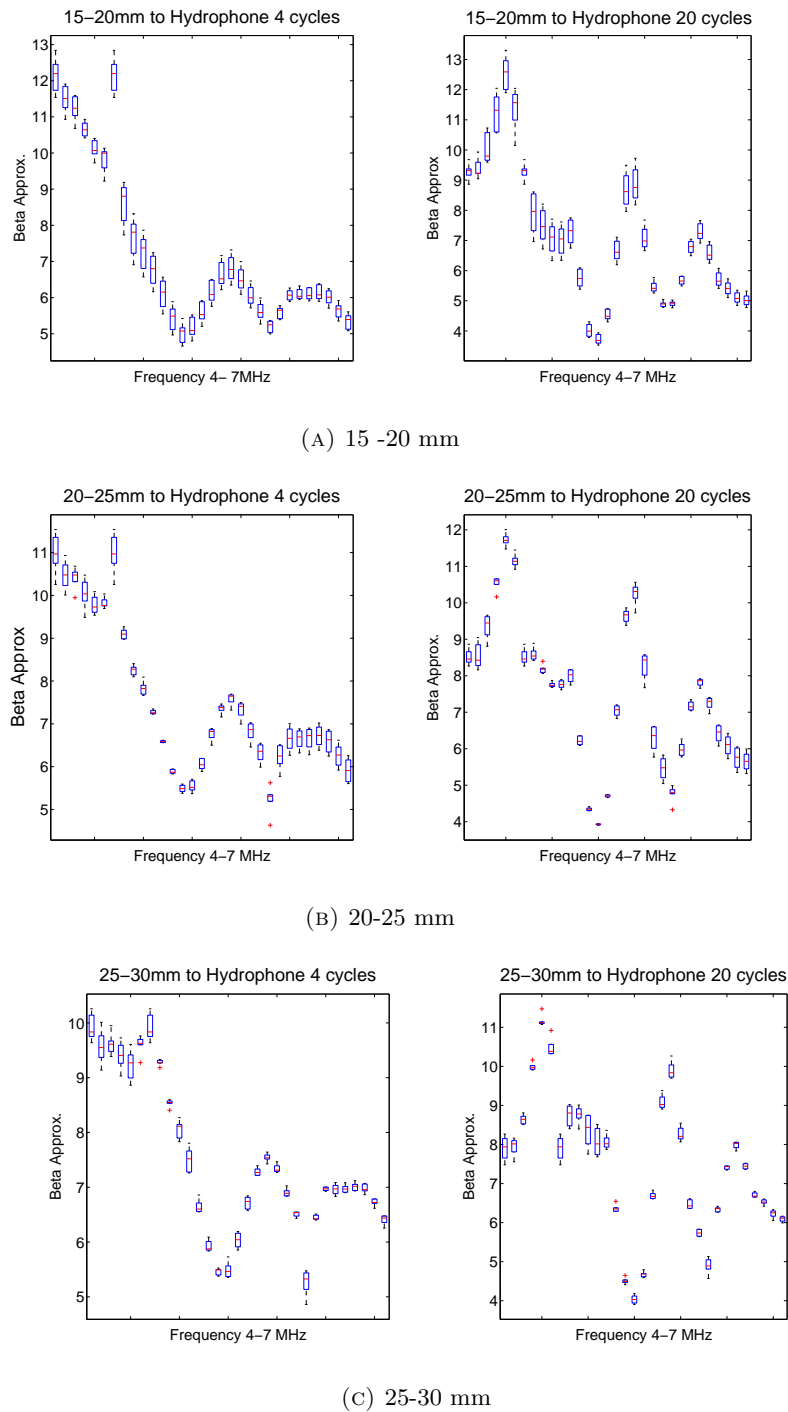


FIGURE 3.6: Box-plot beta versus frequencies from 4 MHz to 7 MHz in steps of 0.1 MHz and 320mV, to different distances.

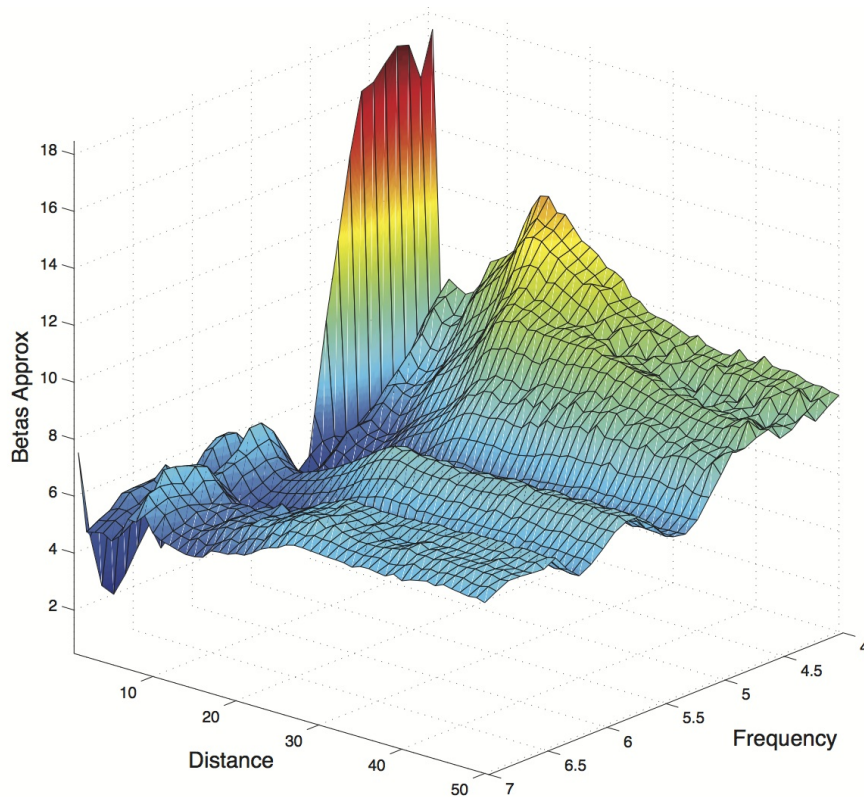


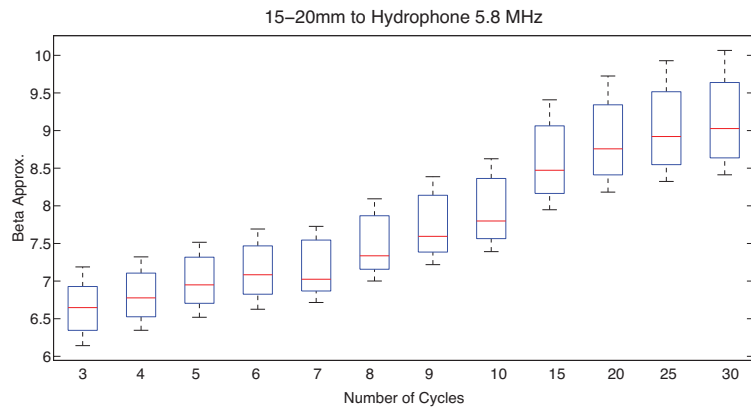
FIGURE 3.7: Surface beta versus frequencies from 4 MHz to 7 MHz in steps of 0.1 MHz and distance from 0.5 mm to 50 mm.

3.2.3 Cycles and Distance

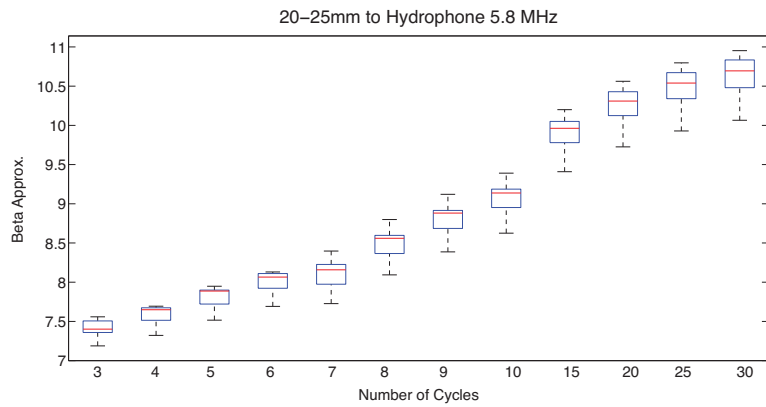
With the fixed excitation level and frequency, in the same way as PMMA, it can be selected the distance between specimen and hydrophone and the number of cycles analysed in which the measure is suitable. In the next three figures it can see, for different distances (15-20, 20-25 and 25-30 mm from specimen) mean and percentiles of beta versus several number of cycles analysed (3-30 cycles), figure 3.8.

Dispersion values decreases with increasing distance to the specimen and increase with the number of cycles due to the interferences specimen-hydrophone. It was selected 4 cycles because with these cycles there is not interferences and the interferences are lower than other number of cycles.

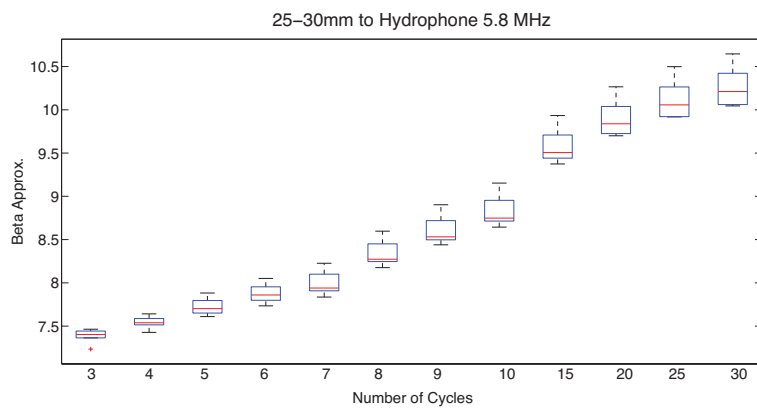
With the last box-plot it can be deduced the appropriate distance to do a feasible measure. This could be fitted in the range of 25-30 mm because in this range, for the number of cycles fixed previously (4 cycles), there are not interferences and the value of beta has lower dispersion than with other distances. Within this range, for a shorter distance



(A) 15–20 mm



(B) 20–25 mm



(C) 25–30 mm

FIGURE 3.8: Box-plot beta versus cycles from 4 MHz to 7 MHz in steps of 0.1 MHz and 320mV, to different distances.

the attenuation is lower than in a longer distance. Therefore it is desirable to choose a distance near to 25 mm.

3.2.4 Selected Parameters

The parameters chosen for CFRP material are shown in the table below for the configuration established in this thesis:

Material	Excitation level (mV)	Frequency (MHz)	Cycles	Distance (mm)
CFRP	320	5.8	4	25-30

TABLE 3.2: Selected parameters to measure the nonlinear parameter in CFRP

Parameters set in the table are advisory and more test have to be done as it is an anisotropic material. Because of the frequencies used, bounces occur in the layers because the wavelength is similar to the thickness of each layer.

3.3 Application of the Semi-Analytical Approach with PMMA Specimen

An application of the semi-analytical approach has been developed in this section in order to validate the method, comparing the results obtained in this method with the results found in literature.

After determining the correct parametric configuration to measure in an immersion tank with PMMA specimen, measures using the defined parameters have been carried out. The scheme used for determining the real parameter β in PMMA is shown in Figure 3.9.

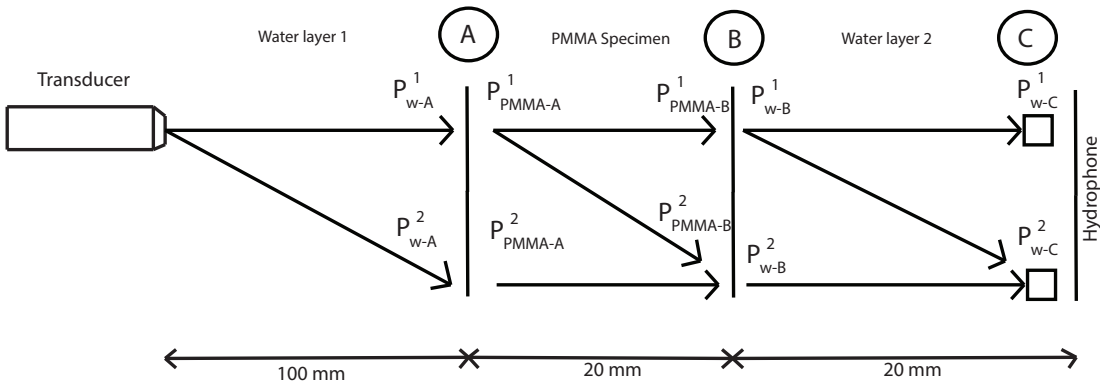


FIGURE 3.9: Semi-analytical approach used to extract the nonlinear material's properties from the measurements in PMMA specimen.

The distance between transducer and PMMA specimen is 100 mm in order to avoid the near field. The near field distance (NF) is determined as follows:

$$NF = \frac{a^2}{\lambda}$$

where $a = 5mm$ is the radius of the transmitter and λ is the sound wavelength.

$$NF = \frac{a^2}{\lambda} = \frac{(5mm)^2}{\frac{1500 \cdot 10^3 mm/s}{5.8 \cdot 10^6 Hz}} = 96.6mm$$

The distance between specimen and hydrophone has been chosen considering the results obtained in Table 3.1.

The values taken to measure in the immersion tank are: excitation level 320 mV, frequency 5.8 MHz, distance specimen-hydrophone 20 mm and 50 cycles were analysed.

The first step is to determine the nonlinear parameter β and geometric attenuation between B and C points with fundamental and second harmonics pressures in this points without PMMA specimen.

$$\begin{aligned}
P_{w-B}^1 &= 8.7868 \cdot 10^{-9} m \\
P_{w-B}^2 &= 1.0985 \cdot 10^{-9} m \\
P_{w-C}^1 &= 7.5771 \cdot 10^{-9} m \\
P_{w-C}^2 &= 1.0131 \cdot 10^{-9} m
\end{aligned}$$

With this values and using the equations 2.12 and 2.15, it will be determined nonlinear parameter β in water and geometric attenuation (Figure 3.10). Water attenuation value was taken from literature ($\alpha = 20 \cdot 10^{-15} \cdot f^2$) [38].

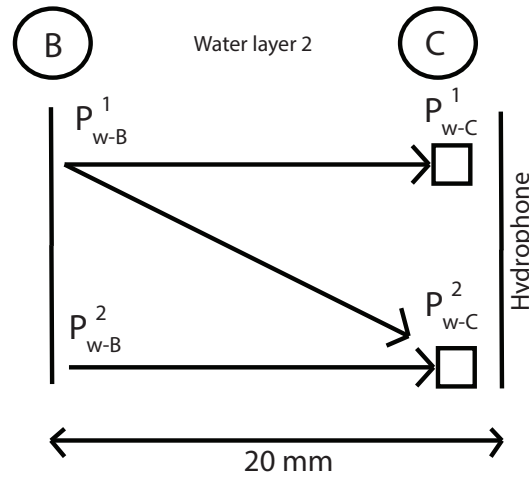


FIGURE 3.10: Determination of the β parameter and geometric attenuation in water layer 2 without specimen.

The values of beta and geometric attenuation are:

$$\begin{aligned}
\beta_w &= 2.5929 \\
\alpha_g^{BC} &= 6.7331 \frac{dB}{m \cdot MHz}
\end{aligned}$$

The nonlinear parameter β obtained in water is ($\beta_w = 2.59$). This value is similar to values found in literature ($\beta_w = 3.5$) [31].

Then, using the same equations (2.12 and 2.15), geometric attenuation between A and B point is obtained without the presence of the specimen. Now, "x" is the distance between A and B.

The values of pressure in A and B points are:

$$\begin{aligned}
P_{w-A}^1 &= 1.0255 \cdot 10^{-8} m \\
P_{w-A}^2 &= 1.1695 \cdot 10^{-9} m \\
P_{w-B}^1 &= 8.7868 \cdot 10^{-9} m \\
P_{w-B}^2 &= 1.0985 \cdot 10^{-9} m
\end{aligned}$$

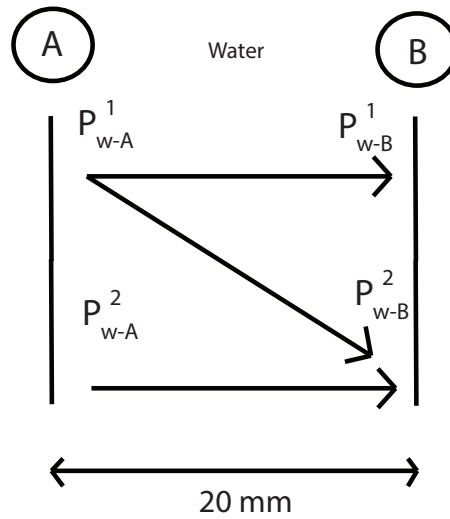


FIGURE 3.11: Determination of the geometric attenuation between A and B points without specimen.

The value of geometric attenuation between A and B points is:

$$\alpha_g^{AB} = 7.0531 \frac{dB}{m \cdot MHz}$$

The next step is to measure the fundamental and second harmonic pressure in C with the presence of the PMMA specimen. This values of pressure are:

$$\begin{aligned} P_{w-C}^1 &= 1.9585 \cdot 10^{-9} m \\ P_{w-C}^2 &= 9.9917 \cdot 10^{-11} m \end{aligned}$$

With this values and the values of nonlinear parameter β in water and geometric attenuation between B and C (previously calculated), it will be determined the amplitude of the fundamental and second harmonic in water and in B point (Figure 3.12), using the equations below:

$$a(0) = \frac{a(x)}{e^{-(\alpha_g + \alpha)x}} = 2.2711 \cdot 10^{-9} m \quad (3.1)$$

$$b(0) = \frac{b(x) - \frac{\beta k^2 a(0)^2}{4(\alpha_g - 2\alpha)} e^{-(2\alpha + 2\alpha_g)x}}{e^{-(4\alpha + \alpha_g)x}} = 1.2897 \cdot 10^{-10} m \quad (3.2)$$

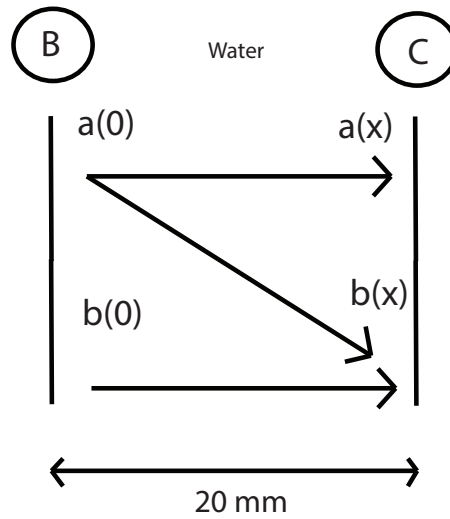


FIGURE 3.12: Determination of the fundamental and second harmonic in B by propagating this values from C to B.

The last step, before reaching the goal, is to obtain the values of the fundamental and second harmonic in A and B in specimen by multiplying this values in water for transmission coefficient water-specimen and specimen-water.

The transmission coefficient water-specimen and specimen-water are:

$$T_{w-s} = \frac{2Z_w}{Z_w + Z_s} = 0.6365 \quad (3.3)$$

$$T_{s-w} = \frac{2Z_s}{Z_w + Z_s} = 1.3635 \quad (3.4)$$

where Z_w and Z_s are the water impedance and the specimen impedance respectively.

Finally, with the values of fundamental and second harmonic in A and B in specimen and taking specimen attenuation from literature and geometric attenuation calculated before between A and B points, the real nonlinear parameter β in specimen, considering viscous and geometric attenuation, is calculated as follows:

$$\begin{aligned} P_{PMMMA-A}^1 &= 6.5277 \cdot 10^{-9} m \\ P_{PMMMA-A}^2 &= 7.4444 \cdot 10^{-10} m \\ P_{PMMMA-B}^1 &= 1.6657 \cdot 10^{-9} m \\ P_{PMMMA-B}^2 &= 9.4592 \cdot 10^{-11} m \end{aligned}$$

$$\beta = \frac{(b(x) - b(0))e^{-(4\alpha_s + \alpha_g)x}(4(\alpha_g - 2\alpha_s))}{k^2 a(0)^2 e^{-(2\alpha_s + 2\alpha_g)x}} = 7.84 \quad (3.5)$$

where "x=20 mm" is the specimen's thickness and $\alpha_s = 4.64 \cdot \frac{dB}{cm}$ is the PMMA attenuation taken from literature [36].

The real nonlinear parameter β in PMMA obtained, removing water contribution and considering viscous and geometric attenuation is very similar to the values found in literature ($\beta_{PMMA} = 7.5$) [5].

Chapter 4

Conclusions and Future Works

Parameters to measure nonlinearity (nonlinear parameter β) in PMMA and CFRP materials have been determined by tests in an immersion tank with water as a medium. The nonlinear parameter β has been determined using the variation of the finite amplitude method with harmonic generation. Using this as a reference, it has been deduced the experimental configuration necessary to measure this nonlinear parameter in a correct and feasible way.

For the PMMA material the experimental configuration was deduced. The separation between the transducer and the specimen was established as 100 mm, whereas the distance between the specimen and the hydrophone was determined in a range of 10-30 mm, but choosing the nearest values to the specimen to avoid problems associated with the attenuation. It was found that the correct number of cycles to get a correct value of the nonlinear parameter was between 50-80 and the frequency was fixed at 5.9 MHz.

On the other hand, in carbon fibre reinforced polymer (CFRP) plate the values of the determined experimental configuration parameters are as follows. The distance between the transducer and the specimen was established at 100 mm, the same as PMMA. This is caused by the influence of the near field that it is wanted to avoid. The separation between the specimen and the hydrophone was determined at a range of 25 mm to 30 mm, choosing the nearest values due to the same reason as well as in PMMA material. The number of cycles in this case descends to 4 cycles, because of the interferences produced inside the material. If it is taken a higher number of cycles, the value of the nonlinear parameter β has too much dispersion. And finally the frequency chosen to measure this material is 5.8 MHz. Due to the material nature, which is very inhomogeneous, anisotropic and random, the configuration parameters in this material must be determined stronger than in this work.

After obtaining the correct configuration to measure the nonlinear parameter β in PMMA and CFRP in an immersion tank, a semi-analytical approach has been developed in order to determine the real nonlinear parameter in any material by removing water contribution and considering viscous and geometric attenuation.

Finally, an application of the semi-analytical approach with PMMA material has been developed in order to validate the method. The result of the nonlinear parameter β in PMMA with this method is 7.84 and this parameter appears consistent with the value found in literature, $\beta = 7.5$ [5].

The future lines of research are listed as below:

- Geometric Attenuation. In this work, geometric attenuation has been considered constant with the distance and it has been found that it is not linear with the distance. The objective is to consider this attenuation nonlinear with the distance.
- Micro-cracks detection. The next step is to generate artificial micro-cracks in these materials simulating very small scale defects in materials that unleash a higher damage. The first step is to generate artificial micro-cracks in PMMA and then determine the nonlinear parameter β . This is because PMMA is a transparent material and the generation of micro-cracks can be observed easily. After analyzing this material, the objective is to determinate crack density in damaged bone basing on the results in PMMA damaged as reference.

Appendix A

Matlab Codes

This appendix provides a summary of the two algorithms developed for the research work presented herein. The codes consist of a collection of Matlab files developed *ad hoc* in conjunction with other Matlab functions. The code to determine the effective nonlinear parameter β in the immersion tank is shown below.

```
1 % Guillermo Rus Carlborg                2013-07-23
2 % Antonio Callejas and Sergio Cantero    2013-11-12
3
4
5 close all; format compact; addpath([pwd '/lib']);
6 addpath([pwd '/lib/acquiris']); f=figure(1);
7 set(f,'doublebuffer','on','Position',[400 200 1000 800]);
8
9
10
11 % Variables Declaration
12
13 rho      = 1e3;                          % density [kg/m^3]
14 c        = 1500;                         % water velocity [m/s]
15 cycles   = 100; nhar=5;                  % (use for 5M,10M)
16 vcycles1 = [3 4 5 6 7 8 9];             % number of cycles
17 vcycles2  = [10:5:30];                   % number of cycles
18 vcycles   = horzcat(vcycles1,vcycles2);  % number of cycles
19
20
21
22 % Frequencies, number of points and cycles of the wind
23
24 freqs1    = [4    4.1  4.2  4.3  4.4  4.5  4.6  4.7  4.8  4.9 ];
25 numbSamples1 = [3200 2940 3150 3010 3080 3150 2990 2820 3120 2940];
```

```

26 cyclewind1 = [320 294 315 301 308 315 299 282 312 294 ];
27
28 freqs2      = [5 5.1 5.2 5.3 5.4 5.5 5.6 5.7 5.8 5.9 6 ];
29 numbSamples2 = [3200 3060 2860 3180 2970 3190 3080 2850 3190 2950 3180];
30 cyclewind2  = [320 306 286 318 297 319 308 285 319 295 318 ];
31
32 freqs3      = [6.1 6.2 6.3 6.4 6.5 6.6 6.7 6.8 6.9 7 ];
33 numbSamples3 = [3050 3100 3150 3200 3120 2970 2680 3060 2760 3150];
34 cyclewind3  = [305 310 315 320 312 297 268 306 276 315 ];
35
36 freqs       =horzcat(freqs1 ,freqs2 ,freqs3);
37 numbSamples =horzcat(numbSamples1 ,numbSamples2 ,numbSamples3);
38 cyclewind   =horzcat(cyclewind1 ,cyclewind2 ,cyclewind3);
39
40
41 dutys       = [.001];
42
43 % voltage at generator (one for each nonlinear energy)
44 volt_waveg = {'320mV' '240mV' '160mV'};
45
46 % voltage range of oscilloscope (same size as above)
47 volt_oscil = [ 16 9.6 6.4 ];
48
49
50
51 % scanning lenght/step [mm] in x (0) axis: left-right (usuario Lx, stepx)
52 Lx = 50; stepx = 1;
53
54 % scanning lenght/step [mm] in y (1) axis: rear-front (usuario Ly, stepy)
55 Ly = 0; stepy = 0;
56
57 % scanning lenght/step [mm] in z (2) axis: vertical (usuario Lz, stepz)
58 Lz = 0; stepz = 0;
59
60
61
62 spacingx= 2e-3*100/2.64 ; % mm to machine units in x/0 axis
63 spacingy= 2e-3*100/2.54 ; % mm to machine units in y/1 axis
64 spacingz= 10e-3*100/2.667; % mm to machine units in z/2 axis
65
66 % waiting time for each mm
67 count=0; pausex=1; pausey=1; pausez=2; pa=.1; pauseread=.5;
68 % load library
69 loadlibrary smc4dll smc4dllImport.h addheader newdef
70
71
72 % +=right direction (x)

```

```

73  calllib('smc4dll','SetDriverData',0,0,0,0,1,4,.001,1,1,0,36000);
74  % +=rear direction (y)
75  calllib('smc4dll','SetDriverData',1,0,0,0,1,4,.001,1,1,0,36000);
76  % +=up direction (z)
77  calllib('smc4dll','SetDriverData',2,0,0,0,1,4,.001,1,1,0,36000);
78
79
80
81  calllib('smc4dll','STEP0'); % needed to initialize
82  waveg_33250_openvisa; % open oscilloscope and wave generator
83  thick=2e-3; % thickness [m]
84
85
86  % sensibility for each frequency
87  f1=[4:.2:7]; f2=[8:.4:14];
88  f=horzcat(f1,f2);
89  s1=[-257.5 -257.2 -257.5 -257.5 -257.5 -257.3 -257.1 -256.9 -257 -257.1
      -257.3 -257.3 -256.8 -256.6 -256.5 -256.5 -256.5 -256.5 -256.5 -256.4
      -255.8 -256 -255.8 -255.8 -256.1 -256.4 -256.5 -256.5 -257.3 -257.2
      -257.6 -258];
90  fq=[4:.1:14];
91  s2=interp1(f,s1,fq);
92  sensibility=10.^(s2./20).*1e6;
93  sensibility1=sensibility(1:40);
94  sensibility2=sensibility(41:2:101);
95
96
97  % Scan
98
99  x=0; % initialize x
100 for nz=1:Lz/(stepz+eps)+1, z=(nz-1)*stepz;
101 for ny=1:Ly/(stepy+eps)+1, y=(ny-1)*stepy;
102 for nx=1:Lx/(stepx+eps)+1, x=(nx-1)*stepx; time1=[];signals1=[];
103
104     % show coordinates
105     disp(sprintf('Coordinates (%d,%d,%d)',x,y,z));
106
107
108  % loop for frequencies
109  for fre = 1:length(freqs); freq=freqs(fre); w=2*pi*freq*1e6;
110  for dut = 1:length(dutys); duty=dutys(dut);
111
112
113  wave_options={sprintf('%1.8fMHz',freq) max(cycles*2,floor(freq*1e3*duty)) '
      5ms'}
114  wind=[cyclewind(fre)/freq/1e6 (0.6776*x+66.50)/1e6];
115

```

```

116
117 % loop for energies
118 for en = 1:length(volt_waveg);
119     waveg_33250_write(volt_waveg{en},wave_options,'0',hVisaw);
120     pause(1); % wait vibration
121     [time1,signal1]=get_acquiris('',wind(1),volt_oscil(en),wind(2),1,1,1,
122         numSamples(fre)); % filename, period, volt, timebase, volt_waveg,
123         wave_options, hVisa
124     pause(.5); signals1(:,nx,fre,dut,en)=signal1(1:2600);
125     times1(:,nx,fre,dut,en)=time1(1:2600);
126     aux=lpcos(signal1,time1,freq*5*1e6);
127     aux(1:floor(60))=0; % to eliminate noise
128     del=raise(aux/75/1.4125e-7/1e3,time1,.1,1);
129
130
131 % if -> to get the delay in the material
132 if fre*dut*en==1
133     dels(nx,ny,nz,fre,dut,en)=del;
134 end;
135     position=find(time1==del);
136
137
138 % loop to measure several cycles
139 for k=1:length(vcycles)
140     a=1;
141     for i=1:(numSamples(fre)-1)-position
142     if (signal1(position+i)<0 & signal1(position+i+1)>0) position1(a)=
143         position+i; a=a+1;
144     end
145     end
146
147     time2=time1(position1(5):(position1(5)+(numSamples(fre)/cyclewind(fre))*
148         vcycles(k)-1));
149     signal2=signal1(position1(5):(position1(5)+10*vcycles(k)-1));
150
151 % convert V-Pa (/75: correct for Acquiris-preamp amplification+impedance)
152 ss=signal2/75/1.4125e-7;
153 fr=0:1/(time2(end)+time2(2)-2*time2(1)):1/(time2(2)-time2(1));
154 fs=abs(fft(ss,length(ss)))/length(ss)*2; p-har=fs(vcycles(k)*(1:nhar)+1);
155
156
157 % getting the phase: fundamental and second harmonic
158 fs_comp=fft(ss,length(ss))/length(ss)*2;

```

```

159     pos_fund=find ( fs==p_har (1) );
160     pos_har=find ( fs==p_har (2) );
161     f_har (1)=atan ( imag ( fs_comp ( pos_fund (1) ) ) / real ( fs_comp ( pos_fund (1) ) ) );
162     f_har (2)=atan ( imag ( fs_comp ( pos_har (1) ) ) / real ( fs_comp ( pos_har (1) ) ) );
163     f_hars (nx, fre , dut , en , k , :)=f_har ;
164
165
166
167     % parameter beta , pressure of five harmonics and variables storage
168     beta=rho*c ^3/(pi*freqs ( fre ) *1e6)/((x+100)/1e3)*(p_har (2) *1.4125e-7/
169     sensibility2 (cont) ) ./ ( p_har (1) *1.4125e-7/sensibility1 (cont) ) .^2
170     p_hars (nx, fre , dut , en , k , :)=p_har ;
171     betas (nx, fre , dut , en , k )=beta ;
172
173
174     % plots
175     subplot (2,1,1) ; plot (time2*1e6, ss/1e3) ; ylabel ( 'Signal [kPa]' ) ; xlabel ( '
176     Time, { \it t } [ \mu s ] ' ) ; axis tight
177     subplot (2,1,2) ; semilogy ( fr/1e6, fs ) ; xlabel ( 'Frequency, { \it f } , [MHz]' ) ;
178     ylabel ( 'Pressure [Pa]' ) ; drawnow ;
179     clear 'time2' ;
180     end ;
181     end ;
182
183     % variables storage for each iteration
184     save ([ filen , '.mat' ] , 'time1' , 'signals1' , 'p_hars' , 'betas' ) ;
185
186
187     % show variables
188     disp ([ 'Saturation risk' , sprintf ( ' % .3f ' , max ( abs ( signals1 ( : , nx , fre , dut , en )
189     ) ) ./ volt_oscil *2 ) ] ) ;
190
191     end ; cont=cont+1 ;
192
193
194     % movement to return to the origin of x, y or z
195
196     if Lx, calllib ( 'smc4dll' , 'MOVE' , 0 , stepx*
197     spacingx ) ; pause ( stepx*pausex+pa ) ; end ;
198     end ; inc=inc+1.3494e-07 ;
199     for nx=1:Lx/(stepx+eps)+1, if Lx, calllib ( 'smc4dll' , 'MOVE' , 0 , -stepx*
200     spacingx ) ; pause ( stepx*pausex+pa ) ; end ; end ; % return to origin of x

```

```

199             if Ly, calllib('smc4dll','MOVE',1,stepy*
                spacingy);pause(stepy*pausey+pa);end;
200 end; for ny=1:Ly/(stepy+eps)+1,if Ly, calllib('smc4dll','MOVE',1,-stepy*
                spacingy);pause(stepy*pausey+pa);end;end; % return to origin of y
201             if Lz, calllib('smc4dll','MOVE',2,stepz*
                spacingz);pause(stepz*pausez+pa);end;
202 end; for nz=1:Lz/(stepz+eps)+1,if Lz, calllib('smc4dll','MOVE',2,-stepz*
                spacingz);pause(stepz*pausez+pa);end;end; % return to origin of z
203
204
205 % final storate of variables
206 save([filename, '.mat'], 'dels', 'p_hars', 'f_hars', 'betas', 'volt_waveg', 'times1
        ', 'signals1');
207
208
209 % Close the oscil communication
210 fclose(hVisaw);

```

The code to determine the real nonlinear parameter β by removing water contribution is shown below.

```

1 % Antonio Manuel Callejas Zafra 2014-05
2
3
4 clear all; clc;
5
6
7 % load harmonics
8
9 load('nl_scan_140611-Water_59MHz_320mV_50cycles.mat');
10
11
12 % initializing variables
13
14 syms alphaw alphag ax bx k beta x a0 b0 ax bx
15
16
17
18 %%%% variables %%%%
19
20 x=(20e-3); % x in [m]
21 k=1/(1500/(5.8e6)); % wavenumber
22 alphaw=(20e-15)*(5.8e6)^2; % water attenuation -> Pinkerton et al.
23 K=1000*1500^2; % compressibility modulus

```

```

24
25
26
27
28 %%% passing Pa to m %%%
29
30     % fundamental harmonic % divide by (K*k)
31     % second harmonic      % divide by (2*K*k)
32
33
34
35
36 % fundamental and second harmonic in water and B
37
38 a0=smooth(p_hars(20,1,1,1,1),100)/(K*k)/(1.4125e-7)*(10.^(-257.3./20).*1e6);
39 b0=smooth(p_hars(20,1,1,1,2),100)/(2*K*k)/1.4125e-7*10.^(-256.2./20).*1e6;
40
41
42
43 % fundamental and second harmonic in water and C
44
45 ax=smooth(p_hars(40,1,1,1,1),100)/(K*k)/1.4125e-7*10.^(-257.3./20).*1e6;
46 bx=smooth(p_hars(40,1,1,1,2),100)/(2*K*k)/1.4125e-7*10.^(-256.2./20).*1e6;
47
48
49 % determination of beta and geometric attenuation in water between B and C
50
51 [Salphag, Sbeta]=solve(ax==a0*exp(-(alphag+alphaw)*x), bx==b0*exp(-(4*alphaw+
    alphag)*x)-((beta*(k^2)*(a0^2))/(-4*(-2*alphaw+alphag)))*exp(-(2*alphaw
    +2*alphag)*x), alphag, beta);
52
53
54 % evaluate beta and geometric attenuation
55
56 alfag=eval(Salphag)
57 BetaReal=eval(Sbeta)
58
59
60
61 % fundamental and second harmonic with PMMA in C
62
63 ax=1.763718284754227e+04/(K*k)/(1.4125e-7)*(10.^(-257.3./20).*1e6)
64 bx=1.585533605947481e+03/(2*K*k)/1.4125e-7*10.^(-256.2./20).*1e6
65
66
67
68 %%% propagated values in B %%%

```

```
69
70 a0=ax/(exp(-(alphaw+alfag)*20*0.001));
71 b0=(bx-((BetaReal*(a0^2)*k^2)/(-4*(alfag-2*alphaw)))*exp(-2*(alphaw+alfag)
      *20*0.001))/(exp(-(alfag+4*alphaw)*20*0.001));
72
73
74
75
76
77 %%%%% values obtained in AB %%%%%
78
79 betaAB=2.5929
80 alphagAB=6.7331;
81
82
83
84
85
86
87 %%%%% Transmission Coefficients %%%%%
88
89 % velocity of sound waves in water and specimen
90
91 c_s=2700; % in [m/s]
92 c_w=1500; % in [m/s]
93
94 % water and specimen density
95
96 rho_s=1190; % in [kg/m^3]
97 rho_w=1000; % in [kg/m^3]
98
99 % impedances
100
101 Zs=c_s*rho_s;
102 Zw=c_w*rho_w;
103
104 % transmission coefficients
105
106 Tsw=2*Zs/(Zs+Zw);
107 Tws=2*Zw/(Zs+Zw);
108
109
110
111
112
113
114
```

```
115 %%% Values of the fundamental and second harmonic in PMMA and in A and B %%
116
117
118 % values of fundamental and second harmonic in water and in A
119
120 aWaterA=9.235167174045643e+04/(K*k)/(1.4125e-7)*(10.^(-257.3./20).*1e6);
121 bWaterA=1.855848309676050e+04/(2*K*k)/(1.4125e-7)*(10.^(-256.2./20).*1e6);
122
123
124 % values of fundamental and second harmonic inside PMMA in A
125
126 aPMMAA=Tws*aWaterA;
127 bPMMAA=Tws*bWaterA;
128
129
130 % values of fundamental and second harmonic in water and in B
131
132 aWaterB=2.271164417141681e-09;
133 bWaterB=1.289727432533617e-10;
134
135
136 % values of fundamental and second harmonic inside PMMA in B
137
138 aPMMAB=aWaterB/Tsw;
139 bPMMAB=bWaterB/Tsw;
140
141
142
143
144
145
146 %%%%%%%%% Determination of the real nonlinear parameter beta %%%%%%%%%
147
148 % initializing variables
149
150 syms alphas betaPMMA
151
152
153 % PMMA attenuation
154
155 alphas=0.8*5.8;
156
157
158 % real nonlinear parameter beta in PMMA
159
```

```
160 [SbetaPMMA]=solve(bPMMAB==bPMMAA*exp(-(4*alphan+alphagAB)*20*0.001)-((
    betaPMMA*(k^2)*(aPMMAA^2))/(-4*(-2*alphan+alphagAB)))*exp(-(2*alphan+2*
    alphagAB)*20*0.001),betaPMMA);
161
162
163 % evaluate beta
164
165 BetaReal=eval(SbetaPMMA)
```

Bibliography

- [1] D Broda, WJ Staszewski, A Martowicz, T Uhl, and VV Silberschmidt. Modelling of nonlinear crack–wave interactions for damage detection based on ultrasound—A review. *Journal of Sound and Vibration*, 333(4):1097–1118, 2014.
- [2] Wesley N Cobb. Finite amplitude method for the determination of the acoustic nonlinearity parameter B/A. *The Journal of the Acoustical Society of America*, 73(5):1525–1531, 1983.
- [3] KE-A Van Den Abeele, Paul A Johnson, and Alexander Sutin. Nonlinear elastic wave spectroscopy (NEWS) techniques to discern material damage, Part I: Nonlinear wave modulation spectroscopy (NWMS). *Research in nondestructive evaluation*, 12(1):17–30, 2000.
- [4] Kenneth W Winkler and Xingzhou Liu. Measurements of third-order elastic constants in rocks. *The Journal of the Acoustical Society of America*, 100(3):1392–1398, 1996.
- [5] Guillaume Renaud, Samuel Callé, Jean-Pierre Remenieras, and Marielle Defontaine. Non-linear acoustic measurements to assess crack density in trabecular bone. *International Journal of Non-Linear Mechanics*, 43(3):194–200, 2008.
- [6] Sylvain Hauptert, Jacques Rivière, Brian Anderson, Yoshikazu Ohara, TJ Ulrich, and Paul Johnson. Optimized dynamic acousto-elasticity applied to fatigue damage and stress corrosion cracking. *Journal of Nondestructive Evaluation*, pages 1–13, 2014.
- [7] J Rivière, G Renaud, RA Guyer, and PA Johnson. Pump and probe waves in dynamic acousto-elasticity: comprehensive description and comparison with nonlinear elastic theories. *Journal of Applied Physics*, 114(5):054905, 2013.
- [8] G Renaud, J Rivière, S Hauptert, and P Laugier. Anisotropy of dynamic acousto-elasticity in limestone, influence of conditioning, and comparison with nonlinear resonance spectroscopy. *The Journal of the Acoustical Society of America*, 133(6):3706–3718, 2013.

- [9] RA Guyer, KR McCall, and Koen Van Den Abeele. Slow elastic dynamics in a resonant bar of rock. *Geophysical research letters*, 25(10):1585–1588, 1998.
- [10] P. A. Johnson. Nonequilibrium nonlinear dynamics in solids: State of art. *Universality of Nonclassical Nonlinearity*, pages 49–69, 2006.
- [11] Sylvain Hauptert, Guillaume Renaud, Jacques Riviere, Maryline Talmant, Paul A Johnson, and Pascal Laugier. High-accuracy acoustic detection of nonclassical component of material nonlinearity. *The Journal of the Acoustical Society of America*, 130(5):2654–2661, 2011.
- [12] K Zacharias, E Balabanidou, I Hatzokos, IT Rekanos, and A Trochidis. Microdamage evaluation in human trabecular bone based on nonlinear ultrasound vibro-modulation (NUVM). *Journal of biomechanics*, 42(5):581–586, 2009.
- [13] MA Breazeale and DO Thompson. Finite-amplitude ultrasonic waves in aluminum. *Applied Physics Letters*, 3(5):77–78, 1963.
- [14] Naoki Matsuda and Shiro Biwa. Frequency dependence of second-harmonic generation in lamb waves. *Journal of Nondestructive Evaluation*, pages 1–9, 2014.
- [15] LK Zarembo and VA Krasil’Nikov. Nonlinear phenomena in the propagation of elastic waves in solids. *Physics-Uspekhi*, 13(6):778–797, 1971.
- [16] F Vander Meulen and L Haumesser. Evaluation of B/A nonlinear parameter using an acoustic self-calibrated pulse-echo method. *Applied Physics Letters*, 92(21):214106, 2008.
- [17] SR Best, AJ Croxford, and SA Neild. Pulse-echo harmonic generation measurements for non-destructive evaluation. *Journal of Nondestructive Evaluation*, pages 1–11, 2013.
- [18] Makoto Fukuda, Morimasa Nishihira, and Kazuhiko Imano. Real time detection of second-harmonic components generated from plastic-deformed metal rod using double-layered piezoelectric transducer. *Japanese Journal of Applied Physics*, 46(7S):4529, 2007.
- [19] Frank A Bender, Jin-Yeon Kim, Laurence J Jacobs, and Jianmin Qu. The generation of second harmonic waves in an isotropic solid with quadratic nonlinearity under the presence of a stress-free boundary. *Wave Motion*, 50(2):146–161, 2013.
- [20] AM Sutin and VE Nazarov. Nonlinear acoustic methods of crack diagnostics. *Radiophysics and quantum electronics*, 38(3-4):109–120, 1995.

- [21] CLE Bruno, AS Gliozzi, M Scalerandi, and P Antonaci. Analysis of elastic non-linearity using the scaling subtraction method. *Physical Review B*, 79(6):064108, 2009.
- [22] Theodore E Matikas. Damage characterization and real-time health monitoring of aerospace materials using innovative NDE tools. *Journal of Materials Engineering and Performance*, 19(5):751–760, 2010.
- [23] Cantrell-J. H. Yost W. T. Na, J. K. Linear and nonlinear ultrasonic properties of fatigued 400Cb stainless steel. *Review of Progress in Quantitative Nondestructive Evaluation*, pages 1347–1352, 1996.
- [24] John H Cantrell and William T Yost. Acoustic harmonic generation from fatigue-induced dislocation dipoles. *Philosophical magazine A*, 69(2):315–326, 1994.
- [25] D Donskoy, A Sutin, and A Ekimov. Nonlinear acoustic interaction on contact interfaces and its use for nondestructive testing. *Ndt & E International*, 34(4):231–238, 2001.
- [26] I Yu Solodov, N Krohn, and G Busse. CAN: an example of nonclassical acoustic nonlinearity in solids. *Ultrasonics*, 40(1):621–625, 2002.
- [27] AL Thuras, RT Jenkins, and HT O’Neil. Extraneous frequencies generated in air carrying intense sound waves. *Bell System Technical Journal, The*, 14(1):159–172, 1935.
- [28] Laszlo Adler and EA Hiedemann. Determination of the nonlinearity parameter B/A for water and m-xylene. *The Journal of the Acoustical Society of America*, 34(4):410–412, 1962.
- [29] Kirk D Wallace, Christopher W Lloyd, Mark R Holland, and James G Miller. Finite amplitude measurements of the nonlinear parameter B/A for liquid mixtures spanning a range relevant to tissue harmonic mode. *Ultrasound in medicine & biology*, 33(4):620–629, 2007.
- [30] AB Coppens, Robert T Beyer, MB Seiden, James Donohue, Frans Guepin, Richard H Hodson, and Charles Townsend. Parameter of nonlinearity in fluids. II. *The Journal of the Acoustical Society of America*, 38(5):797–804, 1965.
- [31] Osterhoudt C. F. Sinha D. N. Pantea, C. Determination of acoustical nonlinear parameter beta of water using the finite amplitude method. 53:1012–1019, 2013.
- [32] Frédéric Plantier, Jean-Luc Daridon, and Bernard Lagourette. Measurement of the B/A nonlinearity parameter under high pressure: Application to water. *The Journal of the Acoustical Society of America*, 111(2):707–715, 2002.

-
- [33] Gong Xiu-fen, Feng Ruo, Zhu Cheng-ya, and Shi Tao. Ultrasonic investigation of the nonlinearity parameter B/A in biological media. *The Journal of the Acoustical Society of America*, 76(3):949–950, 1984.
- [34] WK Law, LA Frizzell, and F Dunn. Ultrasonic determination of the nonlinearity parameter B/A for biological media. *The Journal of the Acoustical Society of America*, 69(4):1210–1212, 1981.
- [35] Pantea C. Sinha N. Sturtevant, B. T. Determination of the acoustic nonlinearity parameter in liquid water up to 250°C and 14 MPa. *Ultrasonics Symposium*, pages 285–288, 2012.
- [36] N. Bochud Parnell W. G. Rus, J. M. L. P. A micro-mechanical approach for bone nonlinear quantitative ultrasound. Part II:Experiment. *Ultrasonics*, 2013.
- [37] S Idjimarene, M Bentahar, R El Guerjouma, and M Scalerandi. Effects of experimental configuration on the detection threshold of hysteretic elastic nonlinearity. *Ultrasonics*, 2013.
- [38] Pikerton. The absorption of ultrasonic waves in liquids and its relation to molecular constitution. *Proceedings of the Physical Society*, Section B(2):129–141, 1949.